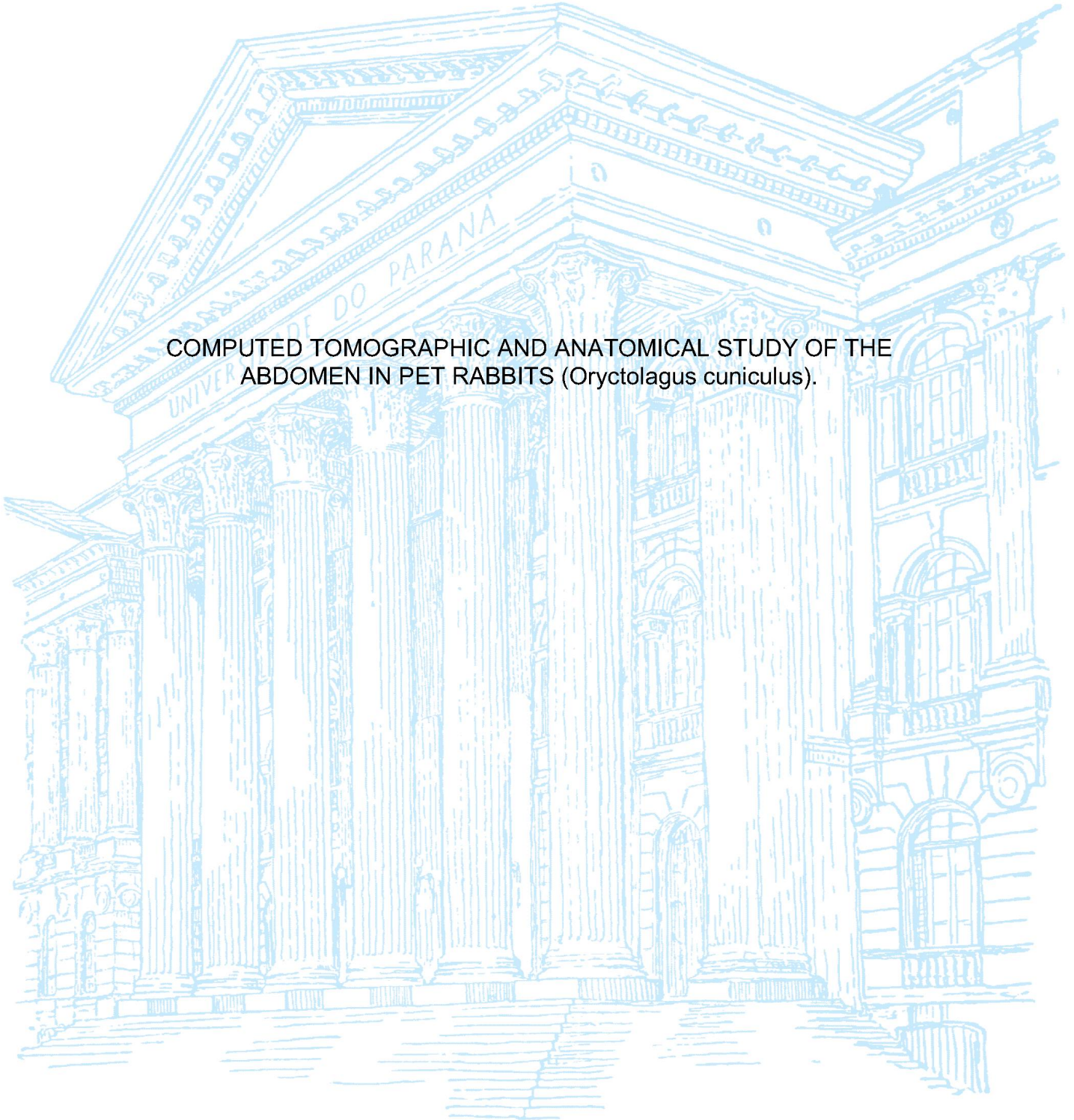


UNIVERSIDADE FEDERAL DO PARANÁ

DANIELLE BUCH

COMPUTED TOMOGRAPHIC AND ANATOMICAL STUDY OF THE
ABDOMEN IN PET RABBITS (*Oryctolagus cuniculus*).



CURITIBA

2021

DANIELLE BUCH

COMPUTED TOMOGRAPHIC AND ANATOMICAL STUDY OF THE
ABDOMEN IN PET RABBITS (*Oryctolagus cuniculus*).

Dissertação apresentada ao curso de Pós-Graduação em Ciências Veterinárias, Setor de Ciências Agrárias, Universidade Federal do Paraná, como requisito parcial à obtenção do título de Mestre em Ciências Veterinárias.

Orientadora: Prof^a. Dr^a. Tilde Rodrigues Froes.

CURITIBA

2021

Buch, Danielle

Computed tomographic and anatomical study of the abdomen in pet rabbits (*Oryctolagus cuniculus*). / Danielle Buch. - Curitiba, 2021.

Dissertação (Mestrado) - Universidade Federal do Paraná. Setor de Ciências Agrárias, Programa de Pós-Graduação em Ciências Veterinárias.

Orientação: Tilde Rodrigues Froes.

1. Diagnóstico por imagem. 2. Lagomorfos. 3. Animais silvestres. 4. Animais exóticos. I. Froes, Tilde Rodrigues. II. Título. III. Universidade Federal do Paraná.



MINISTÉRIO DA EDUCAÇÃO SETOR DE CIÊNCIAS
AGRÁRIAS UNIVERSIDADE FEDERAL DO PARANÁ
PRÓ-REITORIA DE PESQUISA E PÓS-
GRADUAÇÃO PROGRAMA DE PÓS-GRADUAÇÃO
CIÊNCIAS VETERINÁRIAS - 40001016023P3

TERMO DE APROVAÇÃO

Os membros da Banca Examinadora designada pelo Colegiado do Programa de Pós-Graduação em CIÊNCIAS VETERINÁRIAS da Universidade Federal do Paraná foram convocados para realizar a arguição da dissertação de Mestrado de **DANIELLE BUCH** intitulada: **COMPUTED TOMOGRAPHIC AND ANATOMICAL STUDY OF THE ABDOMEN IN PET RABBITS (*Oryctolagus cuniculus*)**,

sob orientação da Profa. Dra. **TILDE RODRIGUES FROES**, que após terem inquirido a aluna e realizada a avaliação do trabalho, são de parecer pela sua **APROVAÇÃO** no rito de defesa.

A outorga do título de mestre está sujeita à homologação pelo colegiado, ao atendimento de todas as indicações e correções solicitadas pela banca e ao pleno atendimento das demandas regimentais do Programa de Pós-Graduação.

CURITIBA, 05 de Março de 2021.

Assinatura Eletrônica

10/03/2021 11:04:18.0

TILDE RODRIGUES FROES

Presidente da Banca Examinadora (UNIVERSIDADE FEDERAL DO PARANÁ)

Assinatura Eletrônica

10/03/2021 10:24:51.0

ROBSON GIGLIO

Avaliador Externo (55001142)

Assinatura Eletrônica

11/03/2021 09:44:05.0

ROGERIO RIBAS LANGE

Avaliador Interno (UNIVERSIDADE FEDERAL DO PARANÁ)

Dedico esta dissertação *in memoriam* a minha maior inspiração, meu herói, meu maior mestre, meu pai Ricardo Buch. Se cheguei aonde cheguei foi devido aos seus ensinamentos como ser humano e professor. O seu exemplo jamais será esquecido assim como o meu amor e admiração por você.

AGRADECIMENTOS

Primeiramente a Deus, por estar sempre ao meu lado, me guiando, confortando e me fortalecendo a cada dia, sei que faz parte do Teu plano colocar as pessoas certas no meu caminho, e no tempo certo. Tudo o que passei e vivi até hoje só foi possível devido as Tuas bênçãos e a Tua permissão.

A minha maravilhosa e companheira mãe Rita que sempre me incentivou a estudar, ensinou a ser uma mulher trabalhadora, a ter garra e lutar por meus objetivos, a ser independente. Que apesar das minhas dúvidas e dos momentos difíceis vividos ao longo desses anos, apoiou e acolheu as minhas decisões e a paixão pela minha profissão. Ao meu pai que embora não esteja mais fisicamente para presenciar mais esta vitória, sei o quão orgulho está de mim e sei que é você quem me dá forças e me conduz no caminho correto, você é certamente meu maior anjo da guarda juntamente com meus amados avós e tios. A vocês meus pais, que desde os primeiros passos até a minha vida adulta, se doaram e se dedicaram ao máximo pelo meu bem-estar e formação, que me suportaram, em todos os sentidos, sem vocês não eu seria nada, minha eterna gratidão.

Ao meu melhor amigo, meu companheiro e grande amor João Eduardo, que me acompanha nessa jornada da vida há lindos 14 anos, sem todo seu amor, sua alegria matinal, paciência, parceria, lealdade, compreensão e acima de tudo apoio nas minhas mais loucas e difíceis decisões, não chegaria aqui tão feliz, motivada e realizada.

A minha incrível e super orientadora, Profa. Tilde Froes, primeiramente por ter acreditado que tinha competência e por ter me impulsionado, mesmo quando eu não tinha certeza de que era capaz de passar por mais esta etapa, e que me despertou uma nova paixão, o ensino. Segundo, por ser uma pessoa tão espetacular, que motiva, não tem preguiça de ensinar e é exemplo diário. E mesmo passando por perrengues em sua própria vida, demonstra uma enorme fé, encara inúmeros desafios e mostra que é possível sim fazer ciência seguindo por este caminho. Por último e não menos importante, por ser somente quem você é, divertida, cheia dos “babados”, com uma risada que é só sua e alegra todo ambiente que passa. Saiba que desde minha decisão em me tornar imaginologista no terceiro ano da faculdade, sua figura serviu de forte inspiração

profissional, pois eu te acompanhava de longe, digamos que “nos bastidores”. No fundo do meu coração, eu sabia que um dia nossa relação seria próxima, e devo tudo a um simples exame de tomografia computadorizada, que nos uniu em 2015 e nunca mais separou. Hoje posso dizer com carinho que tenho uma parceira de vida e profissão, que muito mais que orientada e orientadora, somos amigas. Gratidão é pouco para dizer o quanto é importante para mim!

A minha linda equipe multidisciplinar, André Saldanha, Eloisa Muehlbauer e Elaine Gil, obrigada por aceitar e encarar esse desafio, por serem tão queridos, atenciosos, me ajudar e me acolher logo de cara como parte do *team* UFPR. Sem a pró-atividade de vocês esse estudo não teria dado tão certo, me sinto honrada de poder trocar experiências com pessoas de peso e caráter como vocês.

A Coordenação de Aperfeiçoamento Profissional de Nível Superior (CAPES) pelo auxílio financeiro que permitiu que esse projeto fosse desenvolvido com qualidade e que minha dedicação acadêmica fosse diferenciada.

A toda equipe do LADIV-UFPR, as residentes Thais Landarin, Alana Anselmo e William Prieto por serem queridos, fantásticos e sempre dispostos a me ajudar, a IC, estagiária e monitora Fabiana Freitas pela sua extrema competência e dedicação. As residentes da clínica médica e cirúrgica de animais selvagens, em especial Thaiza de Lima e Rafaella Martini, por me ajudar a conseguir os pacientes para esse projeto. Ao residente Wesley Oliveira da patologia clínica, por colaborar com os exames laboratoriais e deixar esta pesquisa ainda mais completa. Aos outros orientados do curso de pós-graduação: Stephany Lucina, Rafaelle Dea, Marina Silvestre e Vinicius Bentivoglio que direta ou indiretamente, contribuíram na minha ingresso, permanência e conclusão do mestrado. A Camila Marinelli Martins pelos serviços prestados de toda a estatística do projeto.

Aos Professores Rogério R. Lange, Juan Carlos D. Moreno, Marcelo Beltrão Molento, Rafael Felipe C. Vieira e Fabiano M. Ferreira, por ter o privilégio de conhecer seu brilhante trabalho de perto. Pela oportunidade de rever meus professores da graduação, agora em outra e merecida instituição, Peterson T. Dornbusch e Ricardo Vilani. Aos professores da banca, pelo interesse e disponibilidade em participar da minha avaliação, contribuindo com valiosas

observações, jamais esquecerei este lindo momento. Ao curso DZP ministrado pelo professor Thiago Vidotto pelo meu desempenho na escrita científica.

A toda equipe do centro diagnóstico BIONOSTIC por me acolher e ceder a casa ao mundo da pesquisa. A direção e atual gerência (Jeronymo, Vanessa e Cláudia) minha imensa gratidão. A todas as meninas da linha de frente na imagem que passaram por minha vida (Cintia, Jacqueline, Simone, Verena, Marília, Andrea, Beatriz, Chantal, Joyce, Haissa, Yasmin, Giovana, Taysa, Jéssica, Camila e Carolina), cada uma de vocês tem influencia direta na minha formação profissional. A Lye, amiga de longa data, lembro-me das nossas tardes na radiologia quando só queríamos despretensiosamente nos divertir e aprender, hoje com muito orgulho, se tornou excelente cardiologista veterinária, empresária e agora mãe. A todos os anestesistas que me ajudaram ao longo desses anos, mas em especial as amigas Jenifer e Adriana que realizam um trabalho espetacular e admiro demais. Não posso deixar de mencionar, os enfermeiros, estagiários, o serviço de patologia e microbiologia, a recepção, o serviço administrativo, serviço de qualidade, serviço de limpeza e de logística que fazem toda essa enorme engrenagem funcionar, seria injusto da minha parte não mencionar e agradecer cada pessoa que fez parte do lugar o qual passei mais tempo que a minha própria casa por tantos anos.

Aos demais amigos e familiares que acompanharam essa jornada e torceram por mim eu devo mais que tudo, pois ao longo da minha vida os melhores momentos vividos foram ao lado de vocês. Seria impossível citar todo mundo, mas guardo no meu coração e memória o apoio de todos. Contudo, não posso deixar de citar as pessoas mais importantes e que nos últimos anos que foram essenciais: Thais (tem muito de você nesse trabalho!), Bianca, Débora, Dhéri, Danilo, Gabriela, Eduardo, Fabíola, Kharime, Cris, Bárbara, Flávia, Monyque, Cadu, Jéssica. A imensa equipe de profissionais que foram essenciais na minha saúde física e mental nesses últimos anos, e tenho imenso carinho. A minha madrinha Sonia, tia Louiseana e minha segunda família Lilian, João, Julianne, Julia e Bernardo, amo vocês.

Aos amados animais que constituem a melhor parte da natureza. A parte que, mesmo ainda sendo irracional, é inteligente e bondosa. A parte que demonstra afeto sem querer nada em troca. A principal razão a qual eu dedico tanto desde 2004. Meu imenso muito obrigada!

"Fight with determination, embrace life with passion, lose with class and win with boldness, because the world belongs to those who dare, and life is too beautiful to be negligible".

— Charlie Chaplin.

RESUMO

Os avanços nas modalidades de diagnóstico por imagem na medicina veterinária para animais selvagens e exóticos trouxeram melhorias nos cuidados clínicos, cirúrgicos e terapêuticos. Conseqüentemente, a qualidade de vida desses animais também melhorou. Embora existam estudos bem estabelecidos sobre a análise dos resultados em exames radiográficos e ultrassonográficos, não há estudos suficientes avaliando a anatomia de animais de estimação não convencionais pelas modalidades de imagem avançadas, como a tomografia computadorizada (TC). Portanto, não há parâmetros de normalidade para orientar os radiologistas durante a análise dos exames tomográficos. Esta dissertação se concentra no estudo das imagens de TC do abdômen de coelhos de estimação (*Oryctolagus cuniculus*). Especificamente, este estudo consiste em dois capítulos que visam estabelecer referências anatômicas e de imagem do trato urinário (TU) e gastrointestinal (TGI) de tais mamíferos. O primeiro capítulo descreve as técnicas tomográficas utilizadas para obter as imagens do TU, a avaliação das imagens pré e pós administração de contraste via intravenosa e os parâmetros mais importantes na análise dos rins, ureteres, bexiga urinária e uretra de coelhos de estimação. O segundo capítulo descreve os resultados mais relevantes das imagens de TC nos estudos do TGI, que permitem a avaliação de todos os segmentos e o seu trajeto (estômago, duodeno, jejuno, íleo, ceco e cólon) e suas características específicas de ceco (por exemplo, sacculus rotundus e apêndice vermiforme). Esta técnica permite analisar a localização dos órgãos, número e/ou sua simetria, forma, tamanho (em cm e mm), determinar suas margens e limites, o padrão de atenuação medido em Unidades Hounsfield das estruturas, assim como a medida da espessura das paredes dos referidos órgãos e o conteúdo presente no trato gastrointestinal. Ambos os capítulos foram formatados e submetidos como artigos de acordo com os padrões do Journal of Exotic Pet Medicine.

Palavras-chave: Diagnóstico por Imagem. Anatomia seccional. Lagomorfos. Exóticos. Silvestres.

ABSTRACT

Recent advances in diagnostic imaging modalities in veterinary medicine for wild and exotic animals have brought about improvements in clinical, surgical and therapeutic care. Consequently, the quality of life of these animals has also improved. There are many studies reporting the findings of radiographic and ultrasonographic exams in these species. However, there are few reports of anatomical studies using advanced technology, such as computed tomography (CT), in non-conventional pets. This dissertation focuses on the analysis of CT images of the abdomen of pet rabbits (*Oryctolagus cuniculus*). It comprises two chapters reporting anatomical and imaging references of the urinary tract (UT) and gastrointestinal (GI) tract in rabbits. Chapter one describes the tomographic techniques used to obtain UT images, the evaluation of the images pre- and post-administration of intravenous radiological contrast and the key parameters for analysis of the kidneys, ureters, urinary bladder and urethra of pet rabbits. Chapter two describes the most relevant CT imaging findings for GI studies, including the stomach, duodenum, jejunum, ileum, cecum and colon and the specific features of the cecum (e.g., sacculus rotundus and vermiform cecal appendix). With CT it is possible to analyze the location of the organs, number and/or their symmetry, shape, size; to determine their margins and limits, the attenuation pattern (measured in Hounsfield Units) of the structures and measure the thickness of the walls of the GI tract and to determine its contents. The dissertation has been formatted and submitted as articles according to the Journal of Exotic Pet Medicine standards.

Keywords: Diagnosis Imaging. Cross-sectional anatomy. Lagomorphs. Exotics.

LIST OF FIGURES

FIGURE 1 – Post-contrast urinary tract in the dorsal tomographic reconstruction of the rabbit abdominal cavity. (A) Position and shape of the most cranial right kidney and the left kidney (white arrows) and right ureter, visualized as a thin with soft tissue attenuation structure within the fat - not yet filled by contrast (white arrowhead). (B) Ureters (white arrowheads) and urinary bladder (black asterisk) filled with iodine contrast.....28

FIGURE 2 – Transverse tomographic reconstruction of the abdominal cavity in the rabbit, showing the cranial to caudal direction in the post-contrast exam (late phase). (A) Right kidney (white arrow) in relation to L1 (black arrow). (B) Left kidney (white arrow) in relation to L3-L4 (black arrow) (C) Bilateral ureteral position (white arrowheads) at the level of L5. (D) Caudal region of the urinary bladder with visualization of bilateral ureteric insertion (white arrows) and contrast running along the wall (black asterisk).....30

FIGURE 3 – Sagittal tomographic reconstruction of the urinary tract in post-contrast exam (equilibrium phase) of the left (A-D) and right ureter (E-H). (A) Proximal left ureter (white arrow). (B) Left ureter in the cranial third (black arrowhead) to the point of contrast filling defect (white arrow). (C) Ureter in the caudal third (black arrowhead) to the point of contrast filling defect (white arrow). (D) Distal left ureter dorsally located to the urinary bladder and without contrast-enhancement (black arrow). (E) Proximal right ureter (black arrowhead). (F-G) Right ureter displaced dorsally by GI tract showing intimate contact with sublumbar musculature. (H) Right distal ureter at the bladder insertion point (black arrowhead) and the and urinary bladder contrast filling (black asterisk).....31

FIGURE 4 – CT images in arterial post-contrast showing where the wall thickness of the main structures of GI tract was measured indicated by white (stomach) and gray arrows (intestines). (A) Gastric cardia wall (red line); (B) Gastric fundus wall (green line); (C) Gastric body wall (orange line); (D) Gastric pylorus wall (red line); (E) Proximal duodenum wall (green line); (F) Jejunal wall (blue line); (G) Ileal wall (orange line); (I) Cecal wall (orange line); (J) Ascending colon wall (yellow line); (K) Descending colon wall (green line).....46

FIGURE 5 – CT images in arterial post-contrast GI tract showing the length, height and width of stomach and cecum. (A) Largest axes between height and width of stomach (red and yellow lines) in transverse plane; (B) Large axis of the gastric length in dorsal plane (orange line); (C) Perpendicular measurement at 90° angle between gastric length and height in sagittal plane (purple and blue lines); (D) Spinal length (L1 to CFJ) in sagittal plane; (E) Large axis of cecum height (left abdomen) in transverse plane (green line) at level of L4-5; (F) Largest axes between length and width of cecum in dorsal plane (orange and blue lines); (G) Cecal distribution in abdominal cavity, caudal to left kidney in sagittal plane.....47

FIGURE 6 – CT images in dorsal reconstructions of GI tract in arterial post-contrast (soft tissue window). (A) Heterogeneous content in stomach (ingesta), cecum (feces) and fluid content in duodenum (green arrow); (B) Stomach distended by heterogeneous content in stomach, in cecum the same heterogeneous material was observed, and fluid content in small intestine; (C) Distention and gas and ingesta filling stomach and cecum; (D) Location of the sacculus rotundus (yellow arrow) and distal duodenum (green arrow); (E) Location of the vermiform cecal appendix (white arrow).....55

LIST OF GRAPHICS

- GRAPHIC 1** – Bland Altman analysis for interobserver comparison. Concordances with their 95% confidence interval, which show differences from means and deviations (dispersion) of the results in evaluation of left (A) and right (B) pelvis size variable (diameter); and the left (C) and right (D) ureter's size variable (diameter).....33
- GRAPHIC 2** – Coefficient of variation boxplot of measuring variables (length, height and width of cecum and stomach, and the wall thickness of GI tract) between observers expressed in percentage (estimated in mean, interquartile interval, minimum and maximum.....54
- GRAPHIC 3** – Pyloral wall thickness compared to stomach height (distention) showing that there is no correlation between the two variants. The pyloric wall thickness may remain unchanged when the stomach is distended in height. Thus, stomach length is a better parameter for assessing distension of the pylorus.....57

LIST OF TABLES

TABLE 1 – Quantitative and categorical variables analyzed, showing the mean and the standard deviation by observer for US and CT modalities.	28-29
TABLE 2 – Quantitative analysis (mean and standard deviation) and confidence interval 90% (inferior and superior values) of tomographic attenuation measured in Hounsfield Unities (HU) in different regions of rabbit's urinary tract, pre- and post-contrast, considering * $p < 0.05$	31-32
TABLE 3 – Quantitative analysis (mean and standard deviation) and confidence interval 90% (inferior and superior values) of tomographic attenuation measured in Hounsfield Unities (HU) in different regions of rabbit's urinary tract, pre- and post-contrast, considering * $p < 0.05$	32-33
TABLE 4 – Intraobserver analysis (mean and standard deviation) of CT measurements of GI tract, and dimension of the GI tract, expressed as percentages using the coefficient of variations (CV). Considering * $p < 0.05$	51-52
TABLE 5 – Quantitative analysis (mean and standard deviation) of CT measures of the distension GI tract, and wall thickness, and differences between results according to sex in first three columns, and the interobserver analysis in percentage by the coefficient of variations (CV). Considering * $p < 0.05$	52-53
TABLE 6 – Correlation coefficient of CT measurements showing the relationship between distension of the stomach and cecum with wall thickness. Considering * $p < 0.05$	56

LIST OF ABBREVIATIONS

CFJ - Coxofemoral joint
CI - Confidence interval
cm - Centimeter
CT - Computed tomography
CV - Coefficient of variation
DP - Dorsal plane
GI - Gastrointestinal
HU - Hounsfield unities
M - Mean
MAX - Maximum
MD – Median
mm - Millimeter
MIN - Minimum
LK - Left kidney
LP - Left pelvis
LUR - Left ureter
RK - Right kidney
RP - Right pelvis
RUR - Right ureter
TP - Transversal plane
US - Ultrasound or Ultrasonography
UT - Urinary tract
SD - Standard Deviation
SP - Sagittal plane

SUMMARY

1. INTRODUCTION	17
1.1. GENERAL OBJECTIVES.....	21
2. CHAPTER 1: COMPUTED TOMOGRAPHIC FINDINGS OF URINARY TRACT IN RABBITS	22
2.1. ABSTRACT.....	22
2.2 INTRODUCTION.....	23
2.3 MATERIAL AND METHODS.....	24
2.3.1 <i>Animals</i>	24
2.3.2 <i>Computed Tomography Acquisition</i>	25
2.3.3 <i>Statistical Analysis</i>	26
2.4. RESULTS.....	27
2.4.1 <i>Animals</i>	27
2.4.2 <i>Image Interpretation</i>	27
2.4.3 <i>Interobserver Analysis</i>	32
2.5 DISCUSSION.....	34
2.6 CONCLUSION.....	38
2.7 ACKNOWLEDGEMENTS.....	38
2.8 REFERENCES.....	38-40
3. CHAPTER 2: COMPUTED TOMOGRAPHY OF THE GASTROINTESTINAL TRACT IN RABBITS	41
3.1. ABSTRACT	41
3.2. INTRODUCTION	42
3.3. MATERIAL AND METHODS	43
3.3.1 <i>Animals</i>	43
3.3.2 <i>Computed tomography</i>	44
3.3.3 <i>Statistical analyzes</i>	48
3.4. RESULTS.....	48
3.5. DISCUSSION	57
3.6 CONCLUSION	61
3.7 ACKNOWLEDGEMENTS.....	61

3.8 REFERENCES	62-66
4. FINAL CONCLUSIONS.....	67
REFERENCES.....	68-72
APPENDIX.....	73-78

1. INTRODUCTION

Many small mammals are kept as house pets around the world (AVMA 2019, PMFA 2020, ABINPET 2019). Of these, rabbits are the most commonly presented small mammal in exotic clinical practice. They are becoming increasingly popular pets as they require less space, exercise and daily care than dogs and cats.

In Brazil, there are estimated to be 2.3 million small mammals and reptiles kept as pets. Between 2017 and 2018 there was a 5.7% increase in number of small mammal and reptiles kept as pets, while the pet dog population increased by only 3.8% in the same period (ABINPET, 2019).

There is a lot of published information on these small mammal species due to their popularity as experimental laboratory animals, but owners of pet rabbits are now demanding high quality veterinary treatment for their pets. Thus, veterinary practitioners need an evidence-base for treatment of these species to improve their clinical approach.

Rabbits belong to the Lagomorpha order, and are not, as many people think, rodents. The Lagomorpha order comprises two living families: Leporidae (rabbits and hares) and Ochotonidae (pikas). The lagomorphs differ from rodents by virtue of their two pairs of maxillary incisors and a pair of mandibular incisors.

Although there are similarities in the abdominal organs of both orders, rabbits differ, from chinchillas, guinea pigs and rats, in their metabolism, characteristic long ears which are used for thermoregulation, pelvic limbs designed for hopping locomotion, mobility of testicular position, social habits and the fact that they exhibit certain behaviors at set times of day. Certain anatomical features in the GI tract, in particular the intestines, also differ between rabbits and rodents.

The American Rabbit Breeders' Association (ARBA) recognizes 49 breeds of rabbits, many of which are kept as pets. The breeds have widely differing body sizes, conformations, weights, anatomical features and coats (ARBA, 2020). This genetic heterogeneity among these pets is challenging for the veterinary practitioner, who must have the knowledge of a wide range of clinical approaches for these animals.

Most studies of rabbits have been experimental studies using homogenous animals, usually from large breeds, such as the New Zealand or the Standard Chinchilla.

In this study, pet rabbits were mostly represented by the following breeds: Lionheads, Fuzzy and Mini Lops, Netherland dwarfs and other small breeds. They are crepuscular animals, hindgut fermenting herbivores with a large GI tract, and rely on cecotrophic behavior to maintain a healthy and functional digestive system. Rabbits have specific characteristics relating to gastrointestinal digestion and nutrition, e.g., that digestion is carried out by cecal fermentation; and they require a high fiber nutrition. They have two dietary strategies, which are effective during periods of food shortage: the selection of the most digestible foods, and/or the rapid passage of poorly digestible components from the diet, while selectively retaining the most digestible components.

The rabbit stomach is relatively small compared to that of other mammals, such as cats and dogs. It is hook-shaped or "J"-shaped in appearance, located mainly on the left side of the cranial abdomen and is constantly filled and variably distended with aliment and gas. The characteristics of the cardiac orifice prevent vomiting or eructation.

The rabbit intestine is short in comparison with that of other species' (approximately 330cm long) and represents around 12% of the total GI tract volume. It is also usually located in the cranial abdomen. Their duodenum has a relatively small lumen with a slight widening at the end of the bile duct.

The ileum has a dilated terminal part at the ileocecal junction. This thick-walled expansion is called the sacculus rotundus and is more prominent than the other parts of ileum and cecum. The enlargement contains lymphoid tissue. The cecum is the largest and most prominent organ measuring approximately 40cm. It is "C" shaped and located in the medioventral part of the abdominal cavity. It is usually filled with gas, fluids and heterogenous content, containing about 40% of the ingesta. It ends in the "vermiform" cecal appendix (13cm). The colon has an ascending and descending portion, functionally divided into a proximal part (30-50cm) and a longer distal part (80-100cm). The ascending colon in the rabbit is subdivided into four regions: the first two of which are distinguished by their teniaes and haustras. 1) The initial portion of the colon, immediately distal to the cecum, with a surface topography characterized by wart-

like protrusions is 10-20cm in length and endowed with three teniae. 2) The adjoining portion of the colon has one tenia, is about 20-30cm in length and also displays the wart-like protrusions - albeit in a slightly less prominent form. 3) The fusus coli is unique to lagomorphs, corresponding to a short segment of colon, approximately 4-8cm in length, that is free of teniae but exhibits longitudinal folds on its inner aspect and is heavily supplied with ganglion cell aggregates that separate the proximal from the distal colon. These three portions together constitute the proximal colon. 4) The fourth region of the colon, the distal colon, reaches a length of 80–100cm and shows no obvious second-order enlargements on its surface. The distal colon is long with thin walls and runs from the fusus coli to the rectum, usually containing solid feces. Their physiological characteristics differ in each region of the colon. The water content of the ingesta increases slightly during passage through the proximal colon, decreasing in the fusus coli and distal colon.

In general rabbits have a similar urogenital anatomy to other mammals, but with a unique renal physiology which, in abnormal conditions, can result in urinary diseases.

The rabbit kidneys and urinary bladder are similar in shape and location to those of other mammals. Mineral sediment and dense material can be seen as a normal variant in the urinary bladder of rabbits. However, due to the intense excretion of calcium and magnesium, the urinary bladder and kidneys are favored organs for lithiasis formation. The normal serum calcium concentration in rabbits is 30-50% higher than in other mammals, and calcium resorption through the intestinal tract is achieved by passive diffusion and active transport. The excretion of calcium via the gastrointestinal tract occurs independently of serum calcium levels, and kidney excretion or conservation of calcium (according to metabolic needs) is controlled pituitary hormones and by vitamin D. However, vitamin D is less important for calcium metabolism in rabbits than in other mammals. Renal insufficiency consequently leads to a failure of serum calcium regulation. Metabolic changes can be observed in cases of vitamin C insufficiency (scurvy) and fibrous osteodystrophy.

CT scanning uses computer-processed combinations of X-rays, which rotate through 360° around the patient, to produce tomographic (cross-sectional)

images (virtual "slices") of a body. This allows the radiologist to visualize internal organs without the need for a surgery.

CT is a superior technology to ultrasonographic and radiographic evaluation in the diagnosis of some abdominal diseases due its high spatial resolution. Although it is more commonly used in dogs and cats, it is being increasing used for the diagnosis of diseases in other species, especially in small mammals, non-human primates, birds, reptiles and small cetaceans.

CT has a number of disadvantages such as the requirement for general anesthesia to restrain the animal and the cost of the study. However, it is a noninvasive procedure that has a short duration.

Contrast CT is an excellent tool for investigation of kidney glomerular filtration and contrast filling time in the lower urinary tract. In addition, simultaneous evaluation can be made of the location, morphology, size, margins and density or attenuation of these organs with CT. This information can help to establish a prognosis, determine surgical planning and monitor therapeutic interventions.

Prior to the study literature pertaining to anatomy and physiology of lagomorphs was searched to aid the identification of urinary and gastrointestinal structures on the CT images. Measurements were then made of renal length, height and width; renal pelvis dimensions; ureteral diameter; thickness of gastric and intestinal walls; and the luminal diameter of stomach, small intestine, cecum and colon.

A small number of studies have used CT as a research tool for investigation of the abdomen in rabbit abdomens. Mention of CT is made in an article reporting general anatomic imaging (Dilek et al., 2019), in studies of the liver (Dagget et al., 2020; Stamatova-Yovcheva et al., 2013; Stamatova-Yovcheva et al., 2012; Kwata et al., 1984), of the urinary system, especially the kidneys (Kim et al., 2018, Vilalta et al., 2017; Zoller et al., 2017; Kaya et al., 2010, Yonkova et al., 2010; Eken et al., 2009), of the prostate (Dimitrov, 2013, Dimitrov et al., 2011; Dimitrov et al., 2010), intestines (Longo et al., 2018), and in oncological studies (Van Zeeland, 2017; Makey, 2008) and for body surface evaluation (Itoh et al., 2018, Zehnder et al., 2012).

Although there have been many studies of rabbit anatomy, physiology and for determination of the most common diseases, there is still a paucity of

information on the most appropriate diagnostic methods in veterinary non-conventional pet medicine.

1.1 GENERAL OBJECTIVES

The purpose of this study was to identify and describe the anatomic structures of the urinary and gastrointestinal systems in the abdominal cavity of pet rabbits. It provides a guide to the normal anatomy of rabbits visible on CT, with relevant reference values for measurements of both the urinary and GI tracts.

There are many reports of radiographic and ultrasonographic studies (widespread in zoological medicine) of the rabbit abdomen. This study compares the efficiency and reliability of the results obtained by CT examinations with those previously reported in the literature for other modalities. It allows compares findings from other domestic mammalian species (e.g., cats and dogs), to determine if methods described in these species may be also applicable to rabbits.

CT may be a useful alternative imaging modality for clinicians, surgeons and veterinary specialists in the diagnosis of conditions of the urinary and GI tracts in rabbits.

2. CHAPTER 1: COMPUTED TOMOGRAPHIC FINDINGS OF URINARY TRACT IN RABBITS.

2.1 ABSTRACT

Background: The diagnosis of urinary disorders can be challenging in rabbits. Reference values for some characteristics of the urinary tract in rabbits already exist for most imaging modalities. However, there are few studies describing findings using multidetector computed tomography. The aim of this study was to describe the appearance and main features of the urinary tract in healthy pet rabbits using computed tomography (CT). **Methods:** The urinary tract of 23 healthy rabbits was scanned under general anesthesia pre- and post-contrast injection. **Results:** Normal renal length was 3.27-3.43 cm. The ureters were identified in the pre-contrast phase, but better delineated in post-contrast phases. Some focal filling defects were observed in the middle and caudal third of the ureters in more than 50% of the animals on post-contrast exams. There was interobserver disagreement regarding the measurements of renal pelvis, ureters and the exact position of the kidneys in relation to the lumbar vertebrae. **Conclusions and clinical relevance:** This study provides a detailed anatomic description of the urinary tract in rabbits from CT imaging and reference values for further investigations. Gastrointestinal tract distension resulted in less interference with CT examination of urinary tract structures compared to other forms of imaging (radiography or ultrasonography). The exception to this being the path of the ureters.

Keywords: Lagomorphs; Multidetector computed tomography; Sectional anatomy; Urinary system.

2.2 INTRODUCTION

Rabbits are the most popular small mammal kept as a pet in the United States, and, in recent years, there has been increased demand for high quality veterinary care in the species (AVMA, 2018). Rabbits have unique physiological peculiarities such as their calcium metabolism, acid-base balance and glomerular filtration rates^{4,7,10,11,12}. Thus, disorders of the urinary tract are common in rabbits²⁻⁵. Imaging can be useful in the early detection and diagnosis of these diseases, allowing appropriate therapeutic protocols to be instituted and determining prognosis⁵⁻⁷.

Rabbit kidneys are unipapillary (unilobulated and unipyramidal) and have a fibrous capsule associated with fat tissue that surrounds the renal pelvis. They are located in the retroperitoneal space and lie parallel to the aorta and caudal vena cava, with the right kidney positioned more cranially than the left^{4,8,9,10,11,12}. The general appearance of the rabbit kidneys is similar to those of cats in size and shape^{3,5}.

Ureters are thin tubular structures originating in the kidneys and inserting in the dorsocaudal region of the urinary bladder near the bladder neck^{13,33}. The urinary bladder is located in the caudal abdomen and has a pyriform shape. Its shape and size vary according to its distension and, when distended, it can project cranially to the level of the fifth lumbar vertebra⁹⁻¹⁰. The urethra is normally located in the intrapelvic region; it is a short tubular structure (< 20 mm wide) that connects the urinary bladder with the extra-abdominal region. The location of the ureters, urinary bladder, and the urethra in rabbits is the same as other mammals¹.

Computed tomography (CT) is a non-invasive advanced imaging technique that provides detailed information about the morphology of the organs without overlaying by other structures. Although it requires exposure to ionizing radiation and use of sedation or general anesthesia to minimize movement, CT is considered a gold standard technique for investigation of specific abdominal conditions^{5,14,15}. Multidetector computed tomography (MDCT) uses multiple rows of detectors (in place of the single row in conventional CT). This configuration improves volume coverage and scan speed and allows isotropic resolution over a larger volume thus improving image quality compared to conventional CT. CT

provides the most complete examination for evaluation of the urinary tract with optimal anatomic detail of the organs. Furthermore, angiographic and urographic studies can be acquired in the same examination^{5,7,11,16}.

There is limited, or no, literature detailing the CT anatomical description of size, abdominal location, proximity to other organs and evaluation of the kidneys, ureters, urinary bladder and urethra pre- and post-contrast in rabbits¹⁷⁻¹⁸. The aim of this study was to describe the tomographic anatomy of the urinary tract of rabbits, determining the anatomy, topography, dimensions and CT density of the urinary tract in pre- and post-contrast examinations. Variations due to sex and age of the rabbits, and interobserver differences were analyzed to determine the sensitivity of the CT exam.

2.3 MATERIAL AND METHODS

2.3.1 Animals

This study was approved by the CEUA/CSA-UFPR ethical research committee (number 047_2019). Twenty-three pet rabbits (*Oryctolagus cuniculus*) of different breeds, ages, sex, and sexual status (intact or neutered) were enrolled in the study. Owner consent was given for inclusion in the study. The animals underwent a complete physical examination, abdominal ultrasonography and laboratory examinations including complete blood count, serum biochemistry (AST, ALT, GGT, ALP, creatinine, urea, total protein and albumin) and urinalysis (physical-chemical examination and sedimentation). The rabbits included in the analysis were healthy and had no significant abnormalities in any of the tests performed.

Abdominal ultrasonography (US) was performed prior to CT. Ultrasonography was performed without sedation, with the rabbits in dorsal recumbency, using a high-frequency linear transducer (GE Healthcare, LOGIQ 5, Milwaukee, Wisconsin, 12L-RS). The length, echogenicity of the cortex and medulla, renal contours and renal pelvis were evaluated. The urinary bladder was evaluated for morphology, location, degree of distension (low, moderate, marked), contour and wall thickness. The density of the urine was subjectively evaluated by the hyperechoic flecks floating in the anechoic content. Ultrasound

examinations were performed by a single radiologist with experience in sonography in rabbits.

2.3.2 Computed tomography acquisition

The rabbits were sedated with dexmedetomidine (30 µg/kg; Dexdomitor, Zoetis. Abaxis, Inc., Platinum Performance, Inc.), midazolam (1 mg/kg; Dormire, Cristália, Prod. Quím. Farm. Ltda) and butorphanol (0.5 mg/kg; Torbugesic, Zoetis. Abaxis, Inc., Platinum Performance, Inc.) given intramuscularly from a single syringe into the femoris quadriceps muscle. Ten minutes after premedication, a 24G catheter was inserted into the marginal ear vein. Anesthesia was induced with intravenous propofol (Propovan®, Cristália Prod. Quím. Farm. Ltda) at 2 mL/kg/min by manual injection. Anesthesia was maintained with incremental propofol doses to effect. The animals were intubated and maintained using a non-rebreathing circuit with an inspired oxygen fraction of 100% and fresh gas flow of 2 L/min. Rectal temperature was measured pre- and post-tomographic examination, the examination room was maintained at 17°C, and the difference between pre- and post-CT temperature (ΔT) was calculated by the formula: $\Delta T = T_{pre} - T_{post}$.

For the CT exam, the rabbits were positioned in sternal recumbency and a helicoidal, multislice, four-channel tomograph (Alexion, Toshiba America Medical Systems, Otawara, Japan) was used to obtain cross-section images. Images were obtained in 1 mm slice thickness and 1 mm of slice interval (increment). The scanning settings were: 100 kVp and 100 mA, rotation time of 0.75 seconds, rotation speed or 360° scanning, 512 X 512 matrix, and pitch from 1.3 to 1.5. All slices were acquired using the soft tissue algorithm.

Intravenous Iopromide 0.623g (Ultravist® 300. Bayer S.A) was used as the non-ionic iodinated contrast. Iopromide was manually injected at a dose of 300 mg/kg (1.4 mL/kg) over 3 to 4 seconds (Dimitrov, 2012; Kaya, 2010). The rabbits were monitored for any adverse effect of contrast (erythema, anaphylaxis, bradycardia or hypotension) for 30 minutes or until recovery from anesthesia.

After acquisition of the CT images, the images were processed in DICOM (Digital Imaging and Communications in Medicine) format and analyzed by Horos Project DICOM Medical Image Viewer 3.0 software for Mac-OS system. The images were evaluated in the transverse, dorsal and sagittal planes. Roentgen

signs (location, number and symmetry, contours or margins, shape, size and density or attenuation) were used to evaluate the kidneys, ureters, urinary bladder and urethra. The images were observed in pre- and post-contrast examinations and the respective densities in Hounsfield units (HU) were compared. This included: attenuation of the cortex, medulla and renal pelvis; and the attenuation of the urinary bladder at the dorsal and ventral margin in both the pre- and post-contrast phases. In the post-contrast phases, the minimum and maximum attenuation was also measured in each region. The attenuation of the ventral contents of the urinary bladder was compared to the urinary sediment score on US on a scale of 0 to 3 (Table 1). Two radiologists experienced in rabbit imaging analyzed the topography, shape and dimensions of the kidney and dimensions of the renal pelvis and ureters. The density of abdominal fat was analyzed as an indicator of contrast for other organs, and the relationship of the kidneys with the lumbar vertebrae (L2) both in terms of position and size was recorded.

The renal pelvic diameter was measured on cross-sectional images of the mid-portion of the kidneys, on post-contrast exam, in portal and/or late phases, using a linear caliper across the widest point delineated by fat. The ureteral diameter was measured at the widest point in the proximal third, in the portal and late phases of the post-contrast examination. The arterial, portal and late phase times were tabulated and measured in seconds to follow the excretion of contrast.

2.3.3 Statistical analysis

Data were analyzed using SPSS 21.0 (IBM, 2012). Descriptive statistics were performed. Numerical variables were expressed as mean and standard deviation and CI 90%. Categorical variables were analyzed as absolute and relative frequencies.

For the evaluation of normal distribution and frequency of quantitative variables (contrast volume; length of L2 vertebra; kidney length, width, and height; renal pelvis width and ureter diameter) the Shapiro-Wilk test was used.

Interobserver analysis was performed evaluating the following parameters: kidney shape, kidney length in relation to second lumbar vertebral body (L2) in sagittal and dorsal reformatting, and height and width in transverse plane reformatting. The abdominal fat was analyzed, and the observers made a

qualitative estimate of fat accumulation on the scale: little, moderate or marked. The analyzes were performed in the R environment with the "blandr" package (R Core Team, 2019).

2.4 RESULTS

2.4.1 Animals

A variety of rabbit breeds were represented: mixed-breed rabbits (39.13%) and other breeds (60.87%), including Chinchilla, Fuzzy Lop, Rex, Lionhead, Mini Lop, Netherland Dwarf and New Zealand. The majority (69.6%) of rabbits were adult (over 12 months of age) with an average age of 2.5 ± 1.7 years. Five adult animals had no age recorded and were not included in the calculation of the average. The average weight was 2.8 ± 0.7 kg. Sexually intact rabbits represented 69.6% of the animals, 10 females and 6 males. Of the neutered rabbits (30.4%), 4 were female and 3 were male. The mean body temperature before CT examination was 38.6 ± 0.5 °C and 37.4 ± 0.8 °C at the end of the examination, and ΔT was 1.32 ± 0.45 °C.

2.4.2 Image Interpretation

The US parameters of shape, contours, echogenicity of the kidneys and renal pelvis were within the normal range²⁵. Kidney sizes, degree of bladder distension, the presence and scoring of the intraluminal content are summarized in Table 1 for comparison.

The results of the CT exams are summarized in Table 1 and 2. The kidneys were ovoidal with regular contours in 97.8% of the rabbits. The right kidney was located between T13 and L2 and the left kidney between L2 and L5. Minimum and maximum attenuation values were measured on pre- and post-contrast images. The cortex, medulla and renal pelvis were easily differentiated, as was the adipose tissue (hypoattenuating) within the pelvic region and there was an increase in attenuation in all regions analyzed after contrast administration (Figures 1A, 2A and 2B).

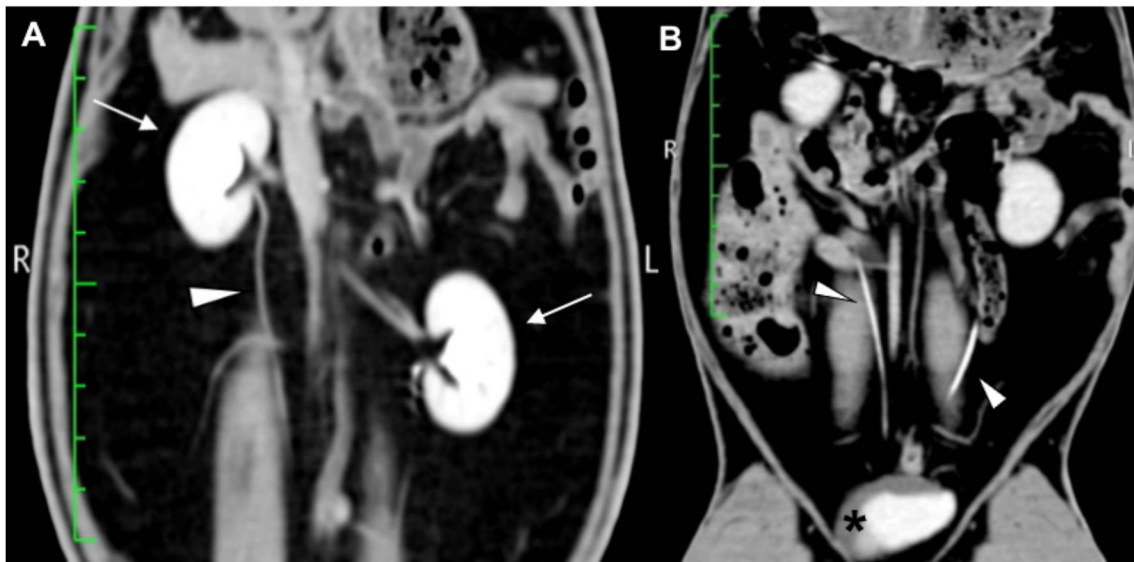


Figure 1. Post-contrast urinary tract in the dorsal tomographic reconstruction of the rabbit abdominal cavity. (A) Position and shape of the most cranial right kidney and the left kidney (white arrows) and right ureter, visualized as a thin with soft tissue attenuation structure within the fat - not yet filled by contrast (white arrowhead). (B) Ureters (white arrowheads) and urinary bladder (black asterisk) filled with iodine contrast.

Table 1. Quantitative and categorical variables analyzed, showing the mean and the standard deviation by observer for US and CT modalities.

Mesures	CT	CI 90% (Inf. and Sup.)	US	CI 90% (Inf. and Sup.)	0	1	2	3
CONTRAST VOLUME (ml)	3.8±1.0	3.2 - 4.3	Not applicable	-	-	-	-	-
VERTEBRAL LENGTH OF L2 (cm)	1.8±0.1	1.7-1.8	Not applicable	-	-	-	-	-
KIDNEY SHAPE								
Ovoid	22	-	22	-	-	-	-	-
Circular and mildly irregular	1	-	1	-	-	-	-	-
US Score - (n. rabbits)		-	-	-	2	5	10	6
RK Length (cm)	3.39 ±0.38	3.1-3,45	3.15 ±0.34	3.02-3.27	-	-	-	-
LK Length (cm)	3.45 ±0.34	3.15-3.55	3.15 ±0.32	2.99-3.1	-	-	-	-
RK Width (cm)	2.40 ±0.20	2.2-2.5	2.34 ±0.23	2.26-2.42				

LK Width (cm)	2.30 ±0.23	2.15-2.4	2.30 ±0.20	2.32-2.37	-	-	-	-
RK Height (cm)	2.0 ±0.20	1.85-2.1	Not measured	-	-	-	-	-
LK Height (cm)	2.1 ±0.20	2.0-2.2	Not measured	-	-	-	-	-
RP Width (mm)	2.3 ±0.3	2.0-2.5	< 3	-	-	-	-	-
LP Width (mm)	2.6 ±0.3	2.0-2.5	< 3	-	-	-	-	-
RUR diameter (mm)	1.3 ±0.4	2.0	Not visualized	-	-	-	-	-
LUR diameter (mm)	1.8 ±0.4	2.0	Not visualized	-	-	-	-	-

RK= Right Kidney, LK= Left Kidney, RP= Right pelvis, LP= Left pelvis, RUR= Right Ureter, LUR= Left Ureter.

The ureters were visualized as tubular structures located in the retroperitoneal space in the region of the mid-caudal abdomen. Their length varied according to the position of the kidneys and urinary bladder, and they had a small caliber of 2 ± 1 mm. In 52% of the rabbits there was a contrast filling defect in the middle or caudal third of the ureter close to the bladder neck. Where contrast filling defects were present, the ureters were still visible due to the surrounding fat which highlighted the thin tubular structure of soft tissue attenuation. However, in these cases measurement of the ureteral diameter was difficult (Figures 1B and 2C). On sagittal sections ureters were visualized as linear, contiguous structures ventral to the lumbar muscles. Contrast filling defects were again visualized in the middle abdominal third (Figures 3B and 3C). Values for ureteral diameter were obtained in neutered (4) and intact (10) females. The mean diameter of the right and left ureters in neutered females was 2.33 ± 0.29 mm and 2.40 ± 0.38 mm respectively; and in intact females the results were 2.32 ± 0.28 mm and 2.37 ± 0.46 mm respectively.

The urinary bladder was located in the caudal abdomen and had a piriform shape, with variable size and distension. It was confined to the intrapelvic region when empty but extended cranially to L4-L5 when distended. In all phases of the tomography exam, it was generally moderately filled with hypoattenuating

material (30 to 60 HU) but, in 18 animals, the ventral sediment was dense and attenuating (200 to 250 HU). The mean value of urinary attenuation in the dorsal bladder on pre-contrast examinations was 43.1 ± 24 HU, and in the ventral region was 126.9 ± 139.2 HU. In late post-contrast examination, the mean value of urinary attenuation in the dorsal bladder region in pre-contrast examination was 66.5 ± 51.2 HU and in the ventral region was 999.2 ± 1133 HU (Figures 1B and 2D).

There was no statistically significant difference in attenuation between age groups for any of the variables ($p > 0.05$).

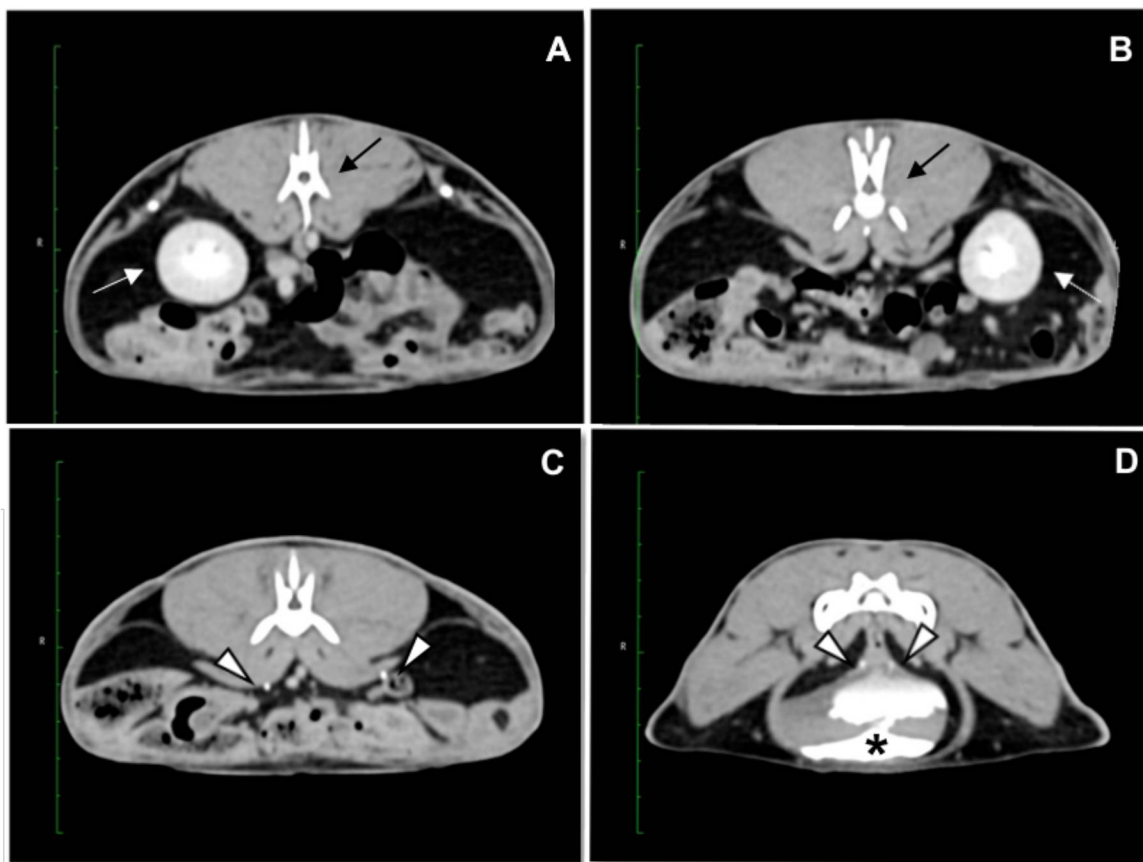


Figure 2. Transverse tomographic reconstruction of the abdominal cavity in the rabbit, showing the cranial to caudal direction in the post-contrast exam (late phase). (A) Right kidney (white arrow) in relation to L1 (black arrow). (B) Left kidney (white arrow) in relation to L3-L4 (black arrow) (C) Bilateral ureteral position (white arrowheads) at the level of L5. (D) Caudal region of the urinary bladder with visualization of bilateral ureteric insertion (white arrows) and contrast running along the wall (black asterisk).

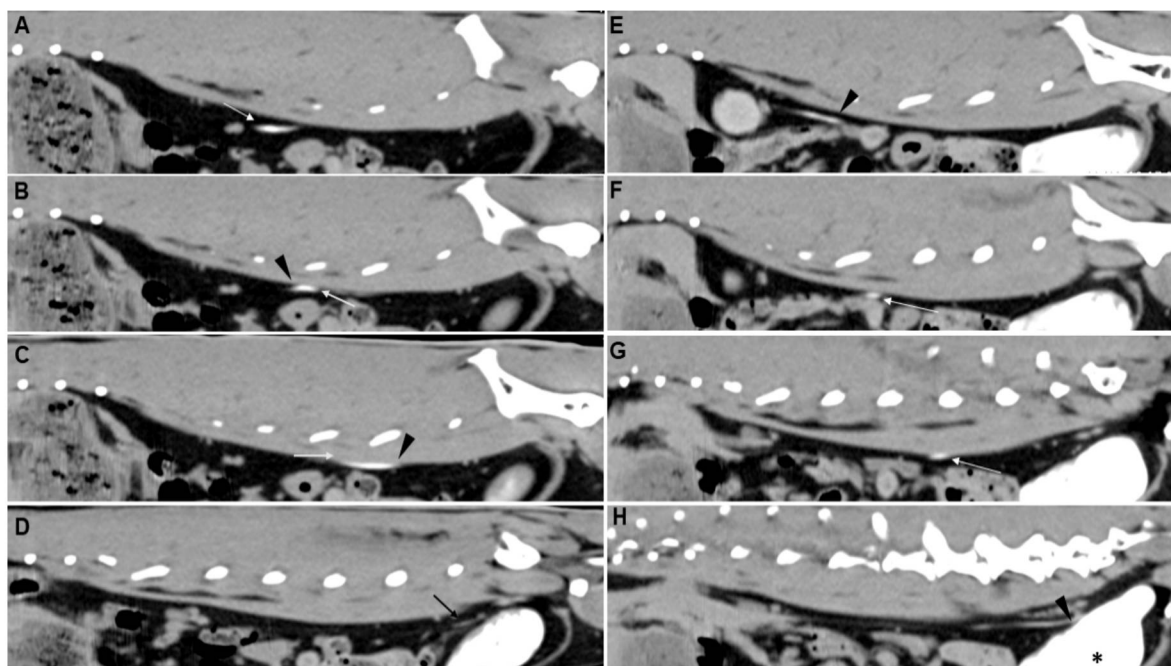


Figure 3. Sagittal tomographic reconstruction of the urinary tract in post-contrast exam (equilibrium phase) of the left (A-D) and right ureter (E-H). (A) Proximal left ureter (white arrow). (B) Left ureter in the cranial third (black arrowhead) to the point of contrast filling defect (white arrow). (C) Ureter in the caudal third (black arrowhead) to the point of contrast filling defect (white arrow). (D) Distal left ureter dorsally located to the urinary bladder and without contrast-enhancement (black arrow). (E) Proximal right ureter (black arrowhead). (F-G) Right ureter displaced dorsally by GI tract showing intimate contact with sublumbar musculature. (H) Right distal ureter at the bladder insertion point (black arrowhead) and the urinary bladder contrast filling (black asterisk).

Table 2. Quantitative analysis (mean and standard deviation) and confidence interval 90% (inferior and superior values) of tomographic attenuation measured in Hounsfield Unities (HU) in different regions of rabbit's urinary tract, pre- and post-contrast, considering * $p < 0.05$.

Region of the Urinary Tract	Tomographic Attenuation (HU)			
	PRE-CONTRAST		POST-CONTRAST	
	Mean/SD	CI 90%	Mean/SD	CI 90%
Min. RK Cortical	27.6±6.3	25.3-29.8	144.6±30.4	133.7-155.4
Max. RK Cortical	51.7±5.7	49.7-53.8	227.6±38.4	213.8-241.3
Min. LK Cortical	28±5.2	26.1-29.9	150.1±33.1	138.3-162
Max. LK Cortical	49.1±7.4	46.5-51.8	226.1±41.6	211.3-241
Min RK Medullar	32.8±7.1	30.2-35.3	213.7±49.2	196.1-231.4
Max. RK Medullar	57.7±9.5	54.2-61.1	410.7±104.4	373.3-448.1
Min. LK Medullar	33.2±6.4	30.9-35.5	223.9±68.7	199.3-248.5
Max. LK Medullar	54.5±9.1	51.2-57.7	400.4±96.8	365.7-435.1
Min. RK Pelvis	-80.8±29.6	(-91.4)-(-64.4)	-42.1±49.9	(-59.9)-(-24.3)
Max. RK Pelvis	33.2 ±20.2*	31.2-44.6	340±172*	278.5-401.6
Min. LK Pelvis	-74.3±27.9	(-84.3)-(-64.4)	-53.6±42.9	(-69)-(-38.3)

Max. LK Pelvis	37.9±18.7*	31.2-44.6	359.8±126.3 *	314.6-405
Ventral region UB	127.6±135.6	79.1-176.2	860.6+1379.2	366.8-1354.4
Dorsal region UB	43.3±23.6	34.9-51.8	63.6±52.6	44.8-82.5

Min. = Minimum, Max.= Maximum, RK = Right Kidney, LK = Left Kidney, UB = Urinary Bladder.

2.4.3 Interobserver analysis

There was high agreement between observers for kidney shape (95.6%), but considerable disagreement regarding the anatomical relationship between the lumbar vertebrae and right (56.5%) and left kidney (47.8%). There was poor agreement (34.8%) between the observers for volume of abdominal fat.

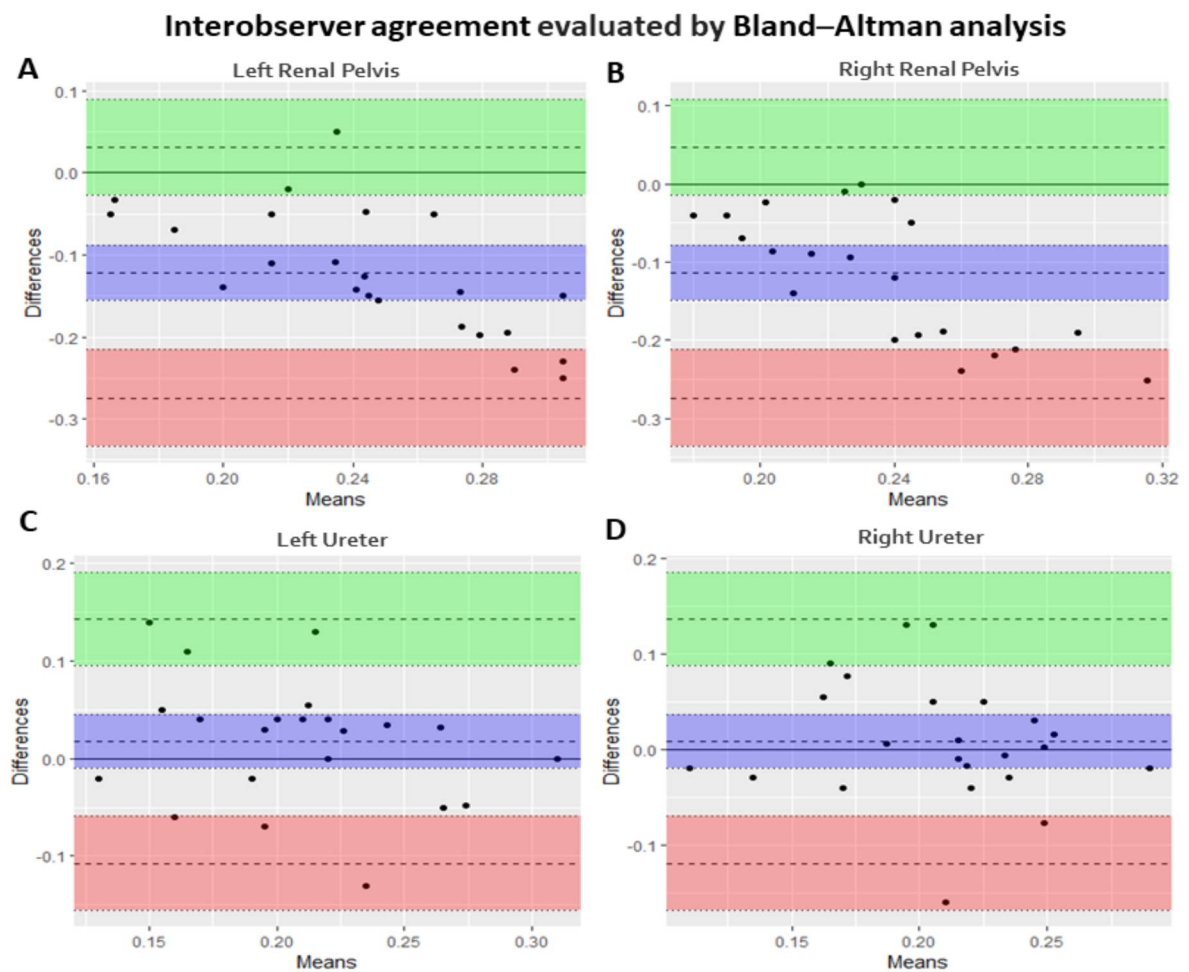
Considering the coefficients of variation in quantitative variables, differences in measurements were observed for the renal pelvis and ureters. In the Bland-Altman analysis, there was no significant difference in interobserver variability regarding length, width or height in kidney measurements. However, there was a statistical difference between the measurements of renal pelvis and ureters (Table 3 and Graphic 1).

Table 3. Interobserver coefficients of variation (CV) and Bland-Altman analysis, showing mean (M), median (MD), minimum (Min) and maximum (Max) values, percentiles, standard deviation (SD), error values of median and standard deviations and confidence interval (CI) of concordance in 95% (inferior and superior).

Interobserver CV	M	MD	Min	Max	25%	75%	SD
VERTEBRAL LENGTH OF L2	3,5%	3,1%	0,0%	17,4%	0,8%	4,4%	3,8%
RK Length	4,2%	3,4%	0,2%	16,7%	1,6%	4,8%	4,0%
LK Length	4,2%	3,6%	0,8%	13,3%	1,6%	5,3%	3,5%
RK Width	8,9%	5,9%	0,3%	30,2%	3,1%	12,9%	7,7%
LK Width	6,1%	6,3%	0,3%	15,3%	1,7%	7,7%	4,1%
RK Height	4,2%	3,2%	0,0%	22,7%	1,5%	6,1%	4,6%
LK Height	3,3%	3,6%	0,0%	8,6%	1,1%	4,7%	2,5%
RP Width	17,3%	12,9%	0,6%	53,9%	4,2%	23,9%	15,8%
LP Width	19,2%	13,5%	0,0%	66,0%	9,9%	25,4%	15,9%
RUR diameter	32,6%	29,6%	0,0%	65,3%	14,9%	54,3%	20,5%
LUR diameter	34,8%	36,9%	6,4%	58,5%	16,4%	48,3%	15,9%

Coefficients of Bland-Altman Analysis					
	Location	Error M	Error SD	CI 95%	
				Inf.	Sup.
Vertebral Length	L2	0.0339	0.115	-0.28	0.346
Renal Length	R	0.0022	0.282	-0.76	0.765

Renal Height	L	0.0909	0.250	-0.59	0.770
	R	0.0352	0.187	-0.47	0.542
Renal Width	L	-0.0048	0.120	-0.33	0.320
	R	0.2574	0.278	-0.50	1.012
Ureter	L	0.2574	0.278	-0.50	1.012
	L	0.0179	0.064	-0.16	0.191
Pelvis	R	0.0084	0.065	-0.17	0.185
	L	-0.1218	0.078	-0.33	0.089
	R	-0.1136	0.082	-0.34	0.108



Graphic 1. Bland Altman analysis for interobserver comparison. Concordances with their 95% confidence interval, which show differences from means and deviations (dispersion) of the results in evaluation of left (A) and right (B) pelvis size variable (diameter); and the left (C) and right (D) ureter's size variable (diameter).

2.5 DISCUSSION

The characteristics of the rabbit digestive tract, specifically its size and variable distension (with ingesta, gas and feces), results in displacement and compression of other organs. This affects analysis of other abdominal organ in many imaging modalities, but by CT the parameters were well evaluated, and these complications almost unaffected the organs studied, with the exception when the GI tract has greater distension, displacing dorsally, promoting contact and sometimes mild compression foci of the ureteral region. This study presents specific tomographic reference values for the rabbit urinary tract. It was possible to define the tomographic location, shape, contours, size and attenuation pattern of the kidneys, renal pelvis, ureters, urinary bladder and urethra in all rabbits. Although the characteristic of the rabbit's digestive tract might impair the organs analysis of the abdominal cavity, CT was efficient in delimiting the rabbit's urinary tract.

This study confirmed the asymmetry in kidney position as reported in the literature^{1,2,3,5,7,9,13,16,17}. Our results suggest that the right kidney is positioned more cranially than the left and may vary topographically with relation to the T13-L1 or L1-L2 vertebrae. The position of the left kidney varied in relation to the L2-L3, L3-L4 and L4-L5 vertebrae. These findings are similar to those observed by Hallmann (2020), but our findings for the right kidney were different from Hristov (2006), who described the location in relation to the T10-T11 intercostal space. When compared to dogs and cats the rabbit kidneys are further apart. This may be related to renal mobility and kidney position in the retroperitoneal space, as well as the amount of fat present in the abdominal cavity. In our study, the disagreement between observers for the exact position of the kidneys in relation to the lumbar vertebrae (for the right kidney 43.5% and for the left kidney 52.2%) may have resulted from either: considering or not considering small vertebral margins that did not include the entire vertebral body; using more than one reconstruction; or not taking into account that the number of thoracic vertebrae may vary in rabbits¹.

There was high observer agreement in the evaluation of the renal shape and in the measurements of the kidneys on CT as compared to ultrasonography. The ovoidal shape can be considered normal and CT allows accurate measurements

of length, width and height of the kidneys. CT's measurements of renal length were higher as those measured by US²⁵. However, the differences between these two techniques were small. Factors such as the better spatial resolution on the CT technique, the absence of transducer pressure (external interference) in CT, and the different positioning of the animal for examination in recumbency in each technique or the muscle relaxation promoted by sedation may explain this. CT appears to be more accurate, both due to the anatomical positioning of the animal and the possibility of multiplanar and three-dimensional evaluations^{6,12,14,15,18,19,20,23,24,32,34}.

In dogs and cats the correlation between kidney length and the vertebral body of L2 is used as a measure of renal size and this may also prove a useful technique in rabbits⁷. On average, rabbit renal length is 1.8 times the length of the vertebral body of L2. There was a high interobserver agreement in determining the kidney size and the vertebral length of L2 by CT. In the radiographic study in rabbits by Dimitrov (2012) the left kidney was reported to be 2.59 times larger, and the right kidney 2.32 times larger than the body of L2. According to Hallman (2020), on radiographic studies, this variation can be between 1.9 and 2.28 cm in Dwarf rabbits and between 2.3 and 2.6 cm for New Zealand rabbits. However, no tomographic references nor breed differences are reported for rabbits.

The attenuation of the kidneys on the pre-contrast examination is similar to the values reported in the literature, between 20-45 HU^{14,32,34}. The renal pelvis was easy to define on CT in the late phase of the examination, but there was disagreement between observers regarding its measurement. The renal pelvis in rabbits is small (< 3 mm) and it is easy to slightly mis-positioned the calipers for measurement, which could generate differences in measurements of the 1 to 2 mm seen between the observers.

It was possible to determine the path and shape of the ureters at a late stage of the post-contrast examination. Mean ureteral diameter was 2 mm. There is no previously reported data for comparison, as normal ureters are not visualized with US or on radiographs^{7,11,16}. The interobserver disagreement in the measurements of ureters may have been due to the absence of a specific measurement point. Although the proximal third was chosen as the site of

measurement of ureteral diameter, each observer may have chosen a different point depending on the ease of identification of the structure.

Although focal filling defects were seen in 52% of the animals, the ureteropelvic and ureterovesical junctions could still be seen. The fact that the ureter runs close to the dorsal spinal musculature can make visualization of the entire ureter difficult, especially in thinner rabbits.

Filling defects were most commonly seen in the middle and caudal third of ureters, cranial to the insertion in the bladder. This is probably the result of the effects of positioning (recumbency) causing lateral and dorsal organ displacement. The higher abdominal fat content in rabbit compared to other species results in displacement of other organs to the periphery reducing the gap between the dorsal abdomen and the abdominal floor. Filling defects are also caused by normal ureteral contractions, which according to Harcourt-Brown (2013) occur approximately every 10 seconds which is a short time compared to the time of CT acquisition. It is important to remember that in adult female rabbits, the uterus lies in ventral abdomen, dorsally to urinary bladder, and the broad ligament may contain large quantities of fat, in our population there were heterogeneity between neutered and intact females, but there were no statistical differences in these groups which could justify the ureteral narrowing. We assume that the degree of intra-abdominal fat regardless of sexual condition may further interfere with ureteral deviation and compression. However, hormonal studies and in a larger group of females is suggested to confirm these findings.

A number of strategies are employed in human CT to minimize the effects of contrast filling defects in ureters. These include changes in recumbency, performing inclination or abdominal compression; use of the contrast medium in bolus and in higher doses (single, split into two or three doses); increased hydration of the patient; use of furosemide; and the performance of imaging in later excretory phases^{26,27,28,29,30,31}. The application of these techniques to rabbits needs further investigation due to the different metabolism and physiology of the species^{2,3,5}.

Shape, contour and distension of the urinary bladder were easily analyzed by CT. An advantage over US was that with CT it was possible to evaluate intrapelvic portions of the bladder and, even when it was poorly distended, the contrast-enhanced examination allowed evaluation of bladder filling^{6,7,8,25}. The degree of

urinary sediment observed at ultrasonography was correlated with the attenuation of the urine in a pre-contrast CT examination. This means that CT can detect differences in rabbits with disorders in calcium metabolism or diseases that result in an increase in urinary density. There are no reference attenuation values for urinary bladder content because it varies according to the density, but it will vary between -10 and 20 HU¹⁴, and should be greater in both dorsal (-19 to 68 HU) and ventral (-18 to 268 HU) regions of the urinary bladder. The urethra can normally be detected on CT due to its enhancement and path and contrast with fat, caudal to the neck of the bladder.

In our study qualitative evaluation of intra-abdominal fat resulted in a classification of little, moderate and marked. The evaluation of the urinary tract, especially the ureteral tract, was facilitated in rabbits that had a moderate accumulation of abdominal fat due to the enhanced contrast promoted by the hypoattenuating material. The fat also provides an interface between the urinary and the gastrointestinal tract, reducing the effects of deviations or compressions. In the interobserver analysis, there was a disagreement of 65.2% in grading the amount of fat, indicating subjectivity in the evaluation, thus we suggest future studies use an alternative analysis to estimate fat.

The limitations of the present study include the difficulty in analyzing breed variations due to the sample size. Although the technique allows better analysis compared with US and radiology, the gastrointestinal physiology of rabbits, which causes a greater filling of hollow viscera (gas, ingesta and feces) can compress and displace some regions of the urinary tract. This can make analysis of the ureter in the middle and caudal portion difficult. Preparation for the CT exam with long dietary fasting and intestinal emptying is not feasible in rabbits, however short-term fasting, associated with use of simethicone or an enema may improve the quality of the images and facilitate the evaluation of the caudal urinary tract^{7,35}.

CT of the urinary tract in rabbits is very useful as it allows identification of all structures of the urinary tract and simultaneous evaluation of a number of parameters on a single slice. Intestinal gas or contents create only minimal interference with evaluations.

2.6 CONCLUSION

Renal length in normal rabbits was determined to be 3.27-3.43 cm on CT. Normal attenuation values for kidney structures and the urinary bladder were established. The ureters can be seen in the pre-contrast phases due to the contrast provided by the retroperitoneal and abdominal fat but are better visualized in post-contrast phases. There was interobserver variation in measurement of ureteral diameter (1.0-2.0 mm). These results represent important reference values for CT studies in normal rabbit urinary tracts.

2.7 ACKNOWLEDGEMENTS

Our sincere thanks go to the owners who agreed to collaborate with this study, to the residents responsible for the cases, to the coordination for the improvement of higher-level personnel (CAPES), to the Bionostic imaging diagnostic center which encourages scientific research and collaborated and made available the computed tomography service. And finally, to Camila Marinelli Martins for her statistical consultancy.

2.8 REFERENCES

1. O'Malley B. Clinical Anatomy and Physiology of Exotic Species: Structure and Function of Mammals, Birds, Reptiles and Amphibians. United Kingdom: Elsevier Ltda. 2005; 8, 173-195.
2. Jenkins JR. Evaluation of the rabbit urinary tract. *J Exot Pet Med.* 2010; 19, 271–279.
3. Harcourt-Brown FM. Diagnosis of Renal Disease in Rabbits. *Veterinary Clinics of North America: Exotic Animal Practice.* 2013;16(1), 145–174. doi:10.1016/j.cvex.2012.10.004.
4. Altuzarra R, Vilalta L, Martorell J, Novellas R, Espada Y. Description of digital fluoroscopic excretory urography in healthy New Zealand rabbits (*Oryctolagus cuniculus*). *Veterinary Record.* 2018; 83(18), 568. doi:10.1136/vr.104618.
5. Reavill DR, Lennox, AM. Disease Overview of the Urinary Tract in Exotic Companion Mammals and Tips on Clinical Management. *Veterinary Clinics of North America: Exotic Animal Practice.* 2020, 23(1),169–193. doi:10.1016/j.cvex.2019.09.003.
6. Mackey EB, Hernandez-Divers SJ, Holland M, Frank P. Clinical Technique: Application of computed tomography in zoological medicine. *J. Exotic Pet Med.* 2008; 17, 198-209.
7. Hallman RM, Brandão J. Diagnostic Imaging of the Renal System in Exotic Companion Mammals. *Veterinary Clinics of North America: Exotic Animal Practice.* 2020; 23(1), 195–214. doi:10.1016/j.cvex.2019.09.004.
8. Moarabi A, Mossalanejad B, Ghadiri A, Borujeni M. Ultrasonographic evaluation of the urinary system in New Zealand White Rabbit and Totai Hare.

- Veterinary Research Forum. 2011;2: 113-120.
9. Dimitrov R, Kostov D, Stamatova K, Yordanova V. Anatomotopographical and morphological analysis of normal kidneys of rabbit (*Oryctolagus cuniculus*), Trakia Journal of Sciences. 2012; 10(2): 79-84.
 10. Dimitrov R, Chaprazov T. An anatomic and contrast enhanced radiographic investigation of the rabbit kidneys, ureters and urinary bladder. Revue Méd Vét. 2012;63 (10): 469-474.
 11. Vilalta L, Altuzarra, R, Espada Y, Dominguez E, Novellas R, Martorell, J. Description and comparison of excretory urography performed during radiography and computed tomography for evaluation of the urinary system in healthy New Zealand White rabbits (*Oryctolagus cuniculus*). American Journal of Veterinary Research. 2017; 78(4), 472–481. doi:10.2460/ajvr.78.4.472.
 12. Zoller G, Langlois I, Alexander K. Glomerular filtration rate determination by computed tomography in two pet rabbits with renal disease. Journal of the American Veterinary Medical Association. 2017; 250(6), 681–687. doi:10.2460/javma.250.6.681.
 13. Sohn J, Couto MA, In: Suckow M A, Stevens K A, Wilson R P. The laboratory Rabbit, Guinea Pig, Hamster and Other Rodents. Elsevier Inc. 2012; 195-213.
 14. Ohlerth S, Scharf G. Computed tomography in small animals – Basic principles and state of the art applications. The Veterinary Journal. 2007; 173(2), 254–271. <https://doi.org/10.1016/j.tvjl.2005.12.014>.
 15. Fields EL, Robertson ID, Brown JC. Optimization of contrast-enhanced multidetector abdominal computed tomography in sedated canine patients. Veterinary Radiology & Ultrasound. 2012;53(5), 507–512. doi:10.1111/j.1740-8261.2012.01950.x.
 16. Fehr M. Computed tomography (CT) and magnetic resonance imaging (MRI). In Diagnostic Imaging of Exotic Pets: Birds, Small Mammals, Reptiles. Eds M. E. Krautwald-Junghanns, M. Pees, S. Reese, T. Tully. Schluetersche Verlagsgesellschaft mbH & Co. KG. 2010, 242-243.
 17. Hristov H, Kostov D, Vladova D. Topographical anatomy of some abdominal organs in rabbits. Trakia Journal of Sciences. 2006; 4, 7-10.
 18. Stamatova KY, Dimitrov R , Toneva Y , Yonkova P, Kostov D, Rusenov A, Uzunova K, Yordanov V. Helical computed tomography application in rabbit liver anatomy: comparison with frozen cross-sectional cuts. Turkish Journal of Veterinary Animal Sciences. 2013; 37, 553–558.
 19. Shojaei B, Vajhi AR, Rostami A, Molaei MM, Arashian I, Hashemnia S. Computed tomographic anatomy of the abdominal region of cat. Iranian Journal of Veterinary Research. 2006; 7(2), 45-52.
 20. Samii VF, McLoughlin MA, Mattoon JS, Drost, WT, Chew DJ, DiBartola SP, Hoshaw-Woodard S. Digital Fluoroscopic Excretory Urography, Digital Fluoroscopic Urethrography, Helical Computed Tomography, and Cystoscopy in 24 Dogs with Suspected Ureteral Ectopia. J Vet Intern Med. 2004; 18, 271–281.
 21. Novelline RA, Rhea JT, Rao P. Helical CT in emergency radiology. Radiology. 1999; 213, 321–339.
 22. Drost, WT. Abdominal computed tomography. In: Proceedings of Western Veterinary Conference: Section Diagnostic Imaging. 2003; February 11–14 Las Vegas, NV.

23. Schwarz T, O'Brien, R: Acquisition Principles. In Schwarz T, Saunders J , editors: *Veterinary computed tomography*, ed 1, Oxford, Wiley-Blackwell. 2011; 5, 9-27.
24. Eken E, Çorumluoglu Ö, Paksoy Y , Besoluk K, Kalayci İ. A study on evaluation of 3D virtual rabbit kidney models by multidetector computed tomography images. *Anatomy*. 2009;3 (1), 41-44. doi: 10.2399/ana.09.009
25. Banzato T, Bellini L, Contiero B, Selleri P, Zotti A. Abdominal ultrasound features and reference values in 21 healthy rabbits. *Veterinary Record*. 2014; 176(4), 101. doi:10.1136/vr.102657
26. Kemper J, Regier M, Begemann PGC, Stork A, Adam G, Nolte-Ernsting C. Multislice Computed Tomography - Urography: Intraindividual Comparison of Different Preparation Techniques for Optimized Depiction of the Upper Urinary Tract in an Animal Model. *Investigative Radiology*. 2005; 40(3),126-133. doi:10.1097/01.rli.0000153023.19104.b1.
27. Dillman JR, Caoili EM, Cohan RH. Multi-detector CT urography: a one-stop renal and urinary tract imaging modality. *Abdominal Imaging*. 2007;32(4),519–529. doi:10.1007/s00261-007-9185-5
28. Roy C, Jeantroux J, Irani FG, Sauer B, Lang H, Saussine C. Accuracy and intermediate dose of furosemide injection to improve multidetector row CT urography. *Clinical Imaging*.2008;3 2(6). 494.doi:10.1016/j.clinimag.2008.08.010.
29. Wang ZJ, Coakley FV, Joe BN, Qayyum A, Meng MV, Yeh BM. Multidetector row CT urography: does supine or prone positioning produce better pelvecalyceal and ureteral opacification? *Clinical Imaging*. 2009; 33(5),369–373. doi:10.1016/j.clinimag.2009.06.001.
30. Hage L, Boll D, Brantner P, Bongartz G, Potthast S. CT-Urography: Comparison of different methods for increasing the intra-abdominal pressure. *International Journal of Diagnostic Imaging*. 2018; 5(1). <https://doi.org/10.5430/ijdi.v5n1p25>.
31. Karavaş E, Gürel S, Kıyan A, Halicioğlu S, Dağistan E. Effect of Prone and Supine Positioning on Computed Tomography Urography Examination. *Urologia Internationalis*. 2018; 101(2), 167–174. doi:10.1159/000490735.
32. Drees RT: Rabbits and Rodents. In Schwarz T, Saunders J, editors: *Veterinary computed tomography*, ed 1, Oxford, Wiley-Blackwell. 2011; 5, 509-516.
33. Kaya M, Bumin A, Sen Y, Aalkan Z. Comparison of Excretory Urography, Ultrasonography-Guided Percutaneous Antegrade Pyelography, and Renal Doppler Ultrasonography in Rabbits with Unilateral Partial Ureteral Obstruction: An Experimental Study. *Kafkas Univ Vet Fak Derg*. 2010; 6(5), 735-741. doi:10.9775/kvfd.2009.1557
34. Schwarz T, Urinary System In: Schwarz T, Saunders J, editors: *Veterinary computed tomography*, ed 1, Oxford, Wiley-Blackwell. 2011; 5. 331-338.
35. da Silva, K.G., de Andrade, C., Sotomaior, C.S. Influence of simethicone and fasting on the quality of abdominal ultrasonography in New Zealand White rabbits. *Acta Vet Scand*. 2017; 59, 48. <https://doi.org/10.1186/s13028-017-0316-x>.

3. COMPUTED TOMOGRAPHY OF THE GASTROINTESTINAL TRACT IN RABBITS.

3.1 ABSTRACT

Background: Gastrointestinal (GI) diseases are common in rabbits. However, although imaging studies can assist clinicians in selecting therapeutic approaches, there are few reports of advanced imaging findings in normal rabbits. Computed tomography (CT) is now recognized as a useful tool in dogs and cats but there are few reports of normal findings on multidetector computed tomography (MDTC) in rabbits. This study describes the CT anatomical appearance of the GI tract in healthy pet rabbits and measurements of the GI tract structures. *Methods:* Twenty-three rabbits were scanned under general anesthesia and the abdominal images were analyzed by experienced radiologists. Location, landmarks and wall thickness of stomach, small and large intestines were determined. Statistical analysis of quantitative and qualitative variables was performed, including the interobserver agreement. *Results:* The wall thickness values were established for stomach (cardia: $3.4 \pm 0.4\text{mm}$; fundus: $1.4 \pm 0.2\text{mm}$; body: $1.4 \pm 0.1\text{mm}$; pylorus: $2.9 \pm 0.5\text{mm}$), duodenum; $1.4 \pm 0.1\text{mm}$; jejunum : $1.2 \pm 0.1\text{mm}$; ileum $1.4 \pm 0.1\text{mm}$, and large intestines (cecum : $1.2 \pm 0.1\text{mm}$; colon ascending: $1.4 \pm 0.3\text{ mm}$ and descending: $1.3 \pm 0.3\text{mm}$). When distended the stomach did not extend beyond the caudal limits of L2, the cecum occupied the ventral abdominal region from T12-T13 to L7-S1, the sacculus rotundus was identified in 11 rabbits. The sacculus rotundus and vermiform cecal appendix was identified only in rabbits where there was minimal large intestinal dilation. *Conclusions and clinical relevance:* In our study it was possible to evaluate regions using CT, that are not normally readily visible on radiographs and US. These results provide new and important reference values for CT studies in normal pet rabbits, mainly of gastric and cecal features, and provide data for further studies in rabbits with GI diseases.

Keywords: Lagomorphs; Multidetector computed tomography; Sectional anatomy; Stomach, Intestines.

3.2 INTRODUCTION

Rabbits are increasingly common pets around the world. They are now the most common exotic mammal presented to veterinary clinics¹⁻⁴ and are common laboratory animals⁵⁻⁶.

Rabbits are hindgut fermenters with a large abdominal cavity. Their gastrointestinal (GI) anatomy and physiology is designed for a high fiber diet^{3,5,10,16-19}. The GI tract in rabbits is relatively long and its contents make up 10% to 20% of body weight^{17,20}. The stomach serves as a reservoir for much of the ingested feed, typically containing 15% of the alimentary tract content. The cardia and pylorus are well developed. The characteristics of the cardiac orifice mean that rabbits are unable to vomit^{5,16-17,20-25}. The small intestine is shorter in rabbits than in other species (around 12% of total gastrointestinal tract volume). The proximal duodenum and terminal portion of the ileum are common sites of obstruction due to luminal narrowing at these points^{5,8,12,17, 20,22-25}.

The cecum is the largest and most prominent organ, occupying almost the entire ventral region of the abdominal cavity of rabbits. It is spiral-shaped and thin-walled comprising 49% of the digestive tract volume and is the primary site of digestible fiber fermentation. The cecum starts from the sacculus rotundus, where there is abundant lymphatic tissue which makes the wall thicker compared to the rest of cecum; and ends in a finger-like, thick-walled and pale sac, called the "vermiform" appendix^{3,17,18,25,26}. The colon is sacculated with bands that divide it into proximal and distal portions. The fusus coli (unique in lagomorphs), a thickened section, corresponds to an area of colon heavily supplied with ganglion cell aggregates, separates the proximal from the distal colon, and produces the two distinct types of rabbit feces (cecotropes and hard feces) which separates the proximal from the distal colon. The distal colon is long, thin walled, and runs from the fusus coli to the rectum^{3, 5,19-24,26-27}.

In rabbits, GI tract problems are frequent causes of morbidity and mortality. The main disorders are hypomotility, gastric stasis, non-obstructive and obstructive ileus, infectious, inflammatory, and mucoid enteropathies, which can result in diarrhea^{2,7-15}. The term Rabbit Gastrointestinal Syndrome (RGIS)

describes a range of clinical signs and concurrent pathological conditions that affect the digestive system. There are many etiologies of RGIS which makes it challenging to diagnose and treat⁹.

Imaging is an essential diagnostic tool for veterinary clinicians working with exotic companion mammals^{13,29,34}. Complete ultrasonographic evaluation of the GI tract in rabbits (e.g., evaluation of the gastric and intestinal wall, following the entire intestinal path, and identification of the intraluminal content) is challenging due to reverberation artifact caused by gas^{13,28-32}. Radiographic examination can be useful in the diagnosis of some GI diseases, but its use is limited when GI syndrome is suspected^{1,9-10,16,34}. Although, the clinical characteristics of the rabbit GI tract are being increasingly studied, there are still few reports correlating imaging findings with clinical disease. Computed tomography (CT) is commonplace in both human patients and other domestic and pet mammals and provides high-quality resolution without superimposition of structures^{4,33,35-36}. There are no published tomographic studies focusing on evaluation of the anatomy of GI tract in rabbits.

This study describes CT examination in rabbits, the tomographic anatomic aspects and reference values for measurements of the GI tract in pet rabbits. It provides new information and compares this with that already described in the literature. Better understanding of the anatomic details of the gastrointestinal tract will improve the diagnostic imaging approach to gastrointestinal disease in rabbits.

3.3 MATERIAL AND METHODS

3.3.1 Animals

Twenty-three pet rabbits (*Oryctolagus cuniculus*) of different breeds, ages, sex, and sexual status (intact or neutered) were enrolled in the study. Owner consent was given for inclusion in the study. The rabbits were healthy and had no significant alterations on any examination performed. This study was approved by the CEUA/CSA-UFPR ethical research committee (number 047_2019).

Rabbits were weighed and abdominal circumference was measured. All rabbits underwent a complete physical examination, abdominal ultrasonography and laboratory examinations including complete blood count and serum

biochemistry (AST, ALT, GGT, ALP, creatinine, urea, total protein and albumin). Abdominal ultrasonography (US) was performed prior to CT by experienced radiologist with the rabbits in dorsal recumbency without sedation using a high-frequency linear transducer (GE Healthcare, LOGIQ 5, Milwaukee, Wisconsin, 12L-RS) to check whether there was any abnormality that impair the CT from being carried out.

3.3.2 *Computed tomography*

Rabbits were sedated with dexmedetomidine (30 µg/kg; Dexdomitor, Zoetis. Abaxis, Inc., Platinum Performance, Inc.), midazolam (1 mg/kg; Dormire, Cristália, Prod. Quím. Farm. Ltda) and butorphanol (0.5 mg/kg; Torbugesic, Zoetis. Abaxis, Inc., Platinum Performance, Inc.) in a single syringe intramuscularly in the pelvic limb. Ten minutes after premedication, a 24G catheter was inserted into the marginal ear vein. Anesthesia was induced with intravenous propofol (2 mL/kg/min manually injected. Propovan®. Cristália Prod. Quím. Farm. Ltda) and maintained with incremental propofol doses to maintain immobilization and muscle relaxation. Animals were intubated and maintained using a non-rebreathing circuit with an inspired oxygen fraction of 100% and fresh gas flow of 2 L/min. Rectal temperature was measured pre- and post-tomographic examination, environmental temperature was maintained at 17°C.

For the CT exam, rabbits were positioned in ventral recumbency and a helicoidal, multislice, four-channel CT scanner (Alexion, Toshiba America Medical Systems, Otawara, Japan) was used to obtain cross-section images. Images were obtained at 1 mm slice thickness, and slice interval (increment). The scanning settings were: 100 kVp and 100 mA, rotation time of 0.75 seconds, 360° scanning, 512 X 512 matrix, and pitch from 1.3 to 1.5. All slices were acquired using the soft tissue algorithm. Intravenous Iopromide 0.623g (Ultravist® 300. Bayer S.A) was used as the non-ionic iodinated contrast. Iopromide was manually injected at a dose of 300mg/kg (1.4 mL/kg) over 3 to 4 seconds (Dimitrov, 2012; Kaya, 2010). Rabbits were monitored for any adverse effect of contrast, e.g., erythema, anaphylaxis, bradycardia or hypotension, for 30 minutes after the procedure or until discharge.

After acquisition of the CT images, images were processed in DICOM (Digital Imaging and Communications in Medicine) format and analyzed by Horos

Project DICOM Medical Image Viewer 3.0 software for Mac-OS system. Images were evaluated in the transverse, dorsal and sagittal planes. Roentgen signs were used to evaluate the stomach, small and large intestines. Images were acquired pre- and post-contrast administration.

The post-contrast arterial phase was selected for image analysis due to increased contrast in the viscera wall (Figure 4). Stomach and intestinal walls thickness were measured (Figure 5). On transverse plane views the wall thickness of different regions of the stomach (cardia, fundus, gastric body and pylorus), of the proximal duodenum (right cranial abdomen after the pylorus), jejunum (left cranial abdomen) and ileum (middle abdominal cranial region or near the ileocecal junction); of the large intestine, composed of the cecum (measured in right abdomen lateral and dorsal margin), ascending colon (in craniomedial position) and descending colon (in caudal abdomen dorsal to the urinary bladder region at level of the last lumbar vertebra). The colon segments were measured where there was better wall delimitation, normally windowing by gas. All thickness measurements were determined in millimeters (mm).

Anatomic landmarks were established, in a transverse plane, as well as the largest height and width axis of the stomach and the height of the cecum in centimeters (cm) were measured (Figure 5A and 5E). In the dorsal plane, the length of the stomach and the length and width of the cecum in centimeters (cm) were measured (Figure 5B and 5F). In the sagittal plane, the height and length of the stomach were measured along an axis through the body from the twelfth intercostal space and the axis bisecting this line and perpendicular to it (Figure 5C).

The distance from the cranial endplate of the first lumbar vertebra (L1) to the region of the hip joint (corresponding to the spinous process of S3) was also measured. The relationship of the GI tract to other structures was also described. The degree of both gastric and cecal distension was assessed relative to the vertebral column. And finally, the predominant material content in stomach and cecum of rabbits was evaluated.

Intraobserver analysis was performed twice with an interval of six months between. Interobserver analysis was performed by two professionals experienced in CT imaging, one of whom was unfamiliar with rabbit imaging. Both observers evaluated the following parameters: height, width and length of the

stomach and cecum distension, thickness of the wall of the stomach, duodenum, jejunum, ileum, cecum and colon.

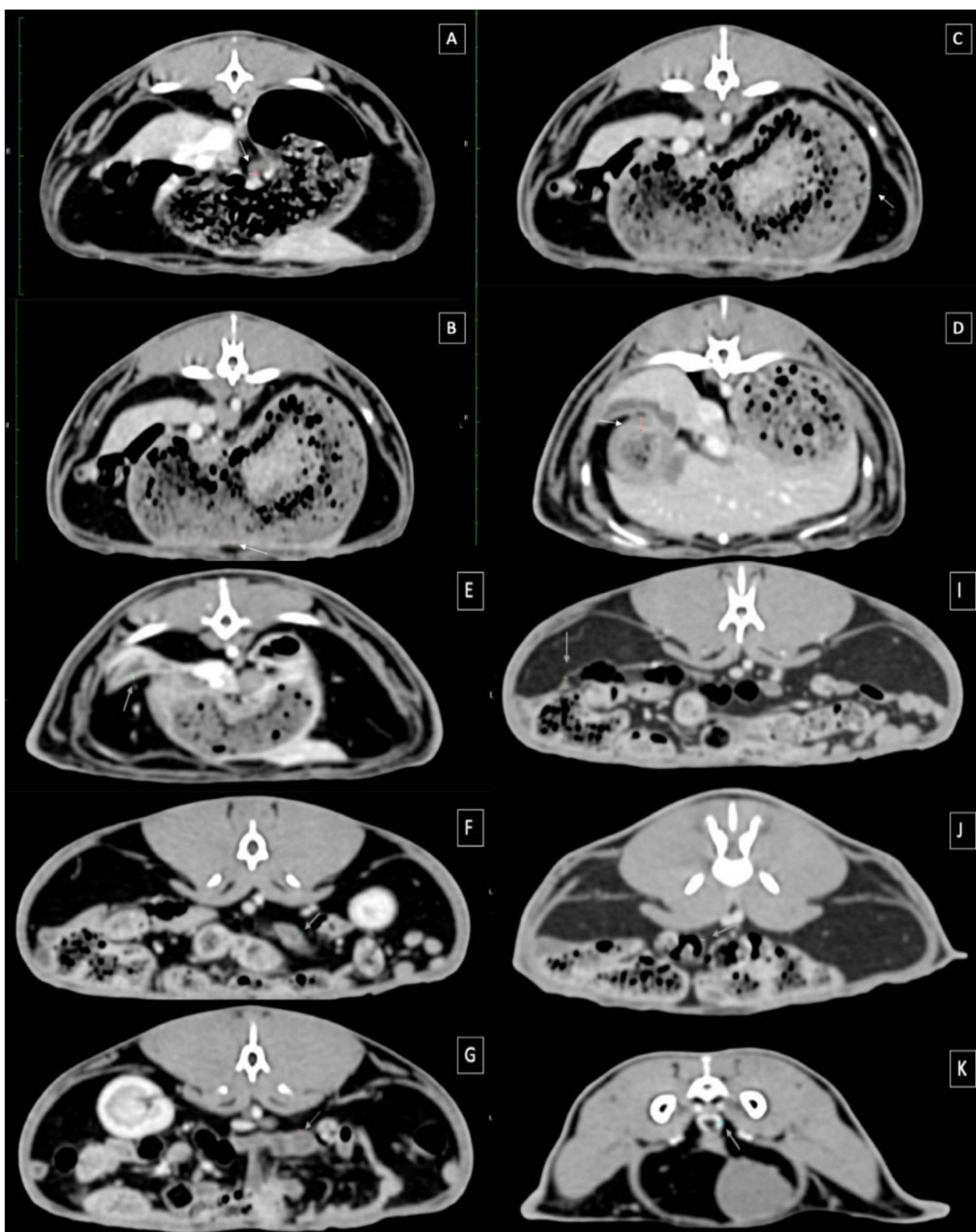


Figure 4. CT images in arterial post-contrast showing where the wall thickness of the main structures of GI tract was measured indicated by white (stomach) and gray arrows (intestines). (A) Gastric cardia wall (red line); (B) Gastric fundus wall (green line); (C) Gastric body wall (orange line); (D) Gastric pylorus wall (red line); (E) Proximal duodenum wall (green line); (F) Jejunal wall (blue line); (G) Ileal wall (orange line); (I) Cecal wall (orange line); (J) Ascending colon wall (yellow line); (K) Descending colon wall (green line).

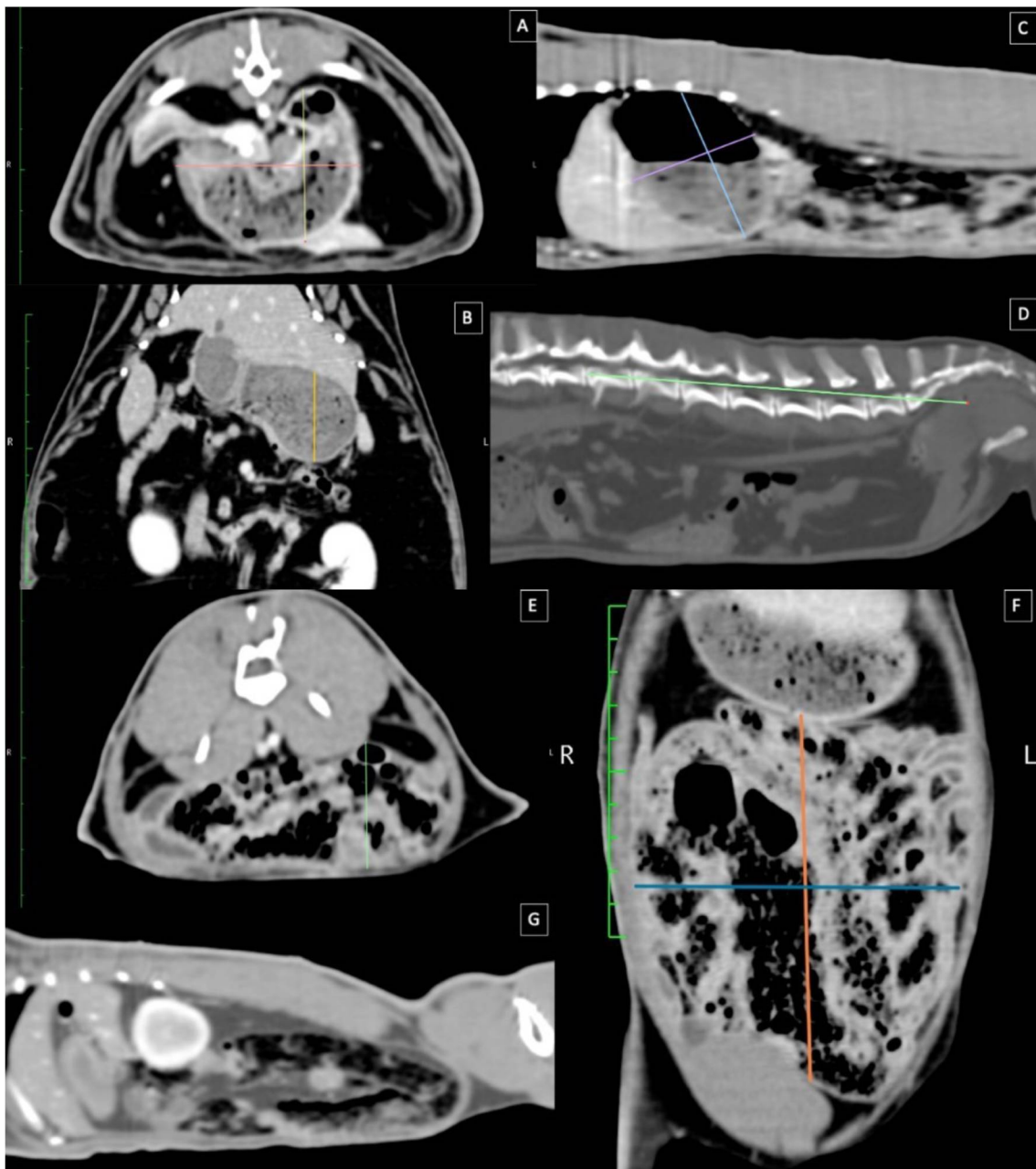


Figure 5. CT images in arterial post-contrast GI tract showing the length, height and width of stomach and cecum. (A) Largest axes between height and width of stomach (red and yellow lines) in transverse plane; (B) Large axis of the gastric length in dorsal plane (orange line); (C) Perpendicular measurement at 90° angle between gastric length and height in sagittal plane (purple and blue lines); (D) Spinal length (L1 to CFJ) in sagittal plane; (E) Large axis of cecum height (left abdomen) in transverse plane (green line) at level of L4-5; (F) Largest axes between length and width of cecum in dorsal plane (orange and blue lines); (G) Cecal distribution in abdominal cavity, caudal to left kidney in sagittal plane.

3.3.3 Statistical analysis

A descriptive analysis of the data was carried out with estimates of mean, and standard deviation. Simple frequencies (n) and relative (%) of the qualitative variables were estimated.

Shapiro-Wilk test was performed to test normal distribution. To check the difference between sexes, Student's T test (parametric variables) and Mann-Witney U test (nonparametric variables) were used. Analyses were considered significant when $p < 0.05$ and they were performed on SPSS 21.0.

Statistical analysis of the intra and interobserver agreement was carried out using the coefficient of variation between the observers which was evaluated for each variable with estimated mean, median, standard deviation, interquartile interval, minimum and maximum. The analyses were carried out using R (R Core Team, 2019) with the "blandr" package (Datta, 2017).

3.4 RESULTS

A variety of breeds were included: mixed-breed (39.2%) and other breeds (60.87%), including Chinchilla, Fuzzy Lop, Rex, Lionhead, Mini Lop, Netherland Dwarf and New Zealand. Average weight was 2.8 ± 0.7 kg. Sexually intact rabbits represented 69.6% of the animals, ten females and six males. Of the seven neutered rabbits (30.4%), there were four females and three males. The mean value of abdominal circumference was 33.5 ± 5.2 cm.

The measurements obtained from CT exams for degree of distension of the stomach and cecum, width, height, and wall thickness of the GI tract segments and the intra and interobserver analysis are summarized in Table 4 and 5. Statistical differences were detected between sexes for abdominal diameter, weight, cardia and descending colon wall thickness. The correlation between distension and wall thickness of stomach and cecum is summarized in Table 6.

The stomach lies in the cranial abdomen, immediately caudal to the liver, with a "U" or "J" shape. The major part (fundus) was located mainly on the left of the midline and the pylorus in the right cranial abdominal. The size and contents of the normal stomach varied considerably. Gastric distention was variable, with cranial extent at T9 (4.39%), T10 (56.52%) and T11 (39.13%) and caudal extent

to T13 (34.78%), L1 (34,78%) and L2 (30,43%). In all rabbits the predominant stomach content was heterogeneous soft tissue opaque ingesta material admixed with gas (with amounts of ingesta and gas ranging from mild to moderate and slight fluid material). The stomach was bounded by the liver, spleen and large intestine. The mucosal surface of the stomach was not characterized by folds (as in dogs and cats). There was no differentiation in the submucosal layer of the stomach, just a line of contrast enhancement delimiting the gastric wall.

Most of the intestines were distributed in the ventral region of the abdominal cavity. The position of the duodenum was relatively constant, located on the right side of the abdomen, similar to its position in cats. The pyloroduodenal region made an acute angle, and the proximal portion of the duodenum was dorsally displaced, contacting the hepatic lobe and the distal portion of duodenum was displaced lateroventrally, close to the right abdominal wall. No duodenal depression or pseudo-ulcerations in duodenal course were observed in the animals evaluated.

The jejunum and ileum were concentrated in the left cranial abdomen due to the cecal position and distention, although the jejunum was more variably distributed. The mean height of the largest small intestinal lumen measured in the sagittal plane was 0.58 ± 0.07 cm. Intestines typically contained fluid and gas attenuating material. In the duodenum, fluid or mucous content was observed in 18 animals (78.26%). A moderate amount of intestinal gas was seen within the jejunum in 13 animals (56.52%) and in the ileum in seven animals (30.43%). In two animals (8.68%) there was no fluid or gas content in small intestinal segments. The jejunum and ileum were very similar in morphology (luminal size, content and wall thickness), only the distal portion of the ileum was distinguishable and was inserted into the cecum in the mid abdomen on the right with the formation of the sacculus rotundus.

The sacculus rotundus was identified in 11 rabbits (47.82%) and was located in the mid abdomen at the level of L4 to L6 (ileocecal junction). It was as a rounded structure with a more prominent wall compared to the rest of the cecum wall. Most rabbits had cecal distension and this compressed and displaced other structures which made consistent visualization of the sacculus rotundus more visible. Depending on the distention and distribution of other parts of the cecum and other intestinal segments, it was positioned adjacent to the midline on right

(nine animals) or left (nine animals). A subtle deviation of the sacculus rotundus was present in 78.26% of the rabbits.

The cecum was large compared to the other intestinal segments, with a "C" shape, and was located in the mid and ventral portion of the abdominal cavity making contact with the lateral and ventral peritoneal wall immediately caudal to the right kidney. The three gyres of cecum were identified. The cecum was the most distended GI segment in the abdomen, occupying a large portion of the middle and caudal abdominal cavity. In 17.39% of the rabbits, the distention of the cecum varied throughout its length, the second and third curvatures being more distended than the first. The cranial margin of the cecum started at the level of T12 and T13 in 30.43% of cases, at L1 to L2 in 26.09%, and at L3 in 8.69%. The caudal margin of the cecum was at the level of L4 in 8.39%, L5 in 13.04%, L6 in 8.39%, L7 in 21.74%, and at the sacrum in 47.82% rabbits. The cecum contained a moderate amount of gas admixed with heterogeneous soft tissue attenuating fecal material in 19 rabbits (82.61%), and in 4 rabbits (17.39%) the intraluminal distension was predominantly gas. The "vermiform" cecal appendix, located in the caudal abdomen, was identified as a finger-like structure in ten rabbits (43.48%).

The observers were able to identify and follow all segments of the colon. The colon began at the cecocolic junction, which was indistinct in wall layering, but the corrugated appearance of the proximal colon and its arrangement made it easier to find its junction with the large intestine. The ascending colon began in the midabdominal cavity, but was sometimes positioned slightly to the left side, dorsal to the insertion of ileum. The first segment of the colon, ampulla coli, could not be distinguished from other segments on CT images. The ascending colon was located in the right caudal midabdominal region at the level of L5, surrounded by a cecum loop. The transverse colon ran across the abdomen and continued as the descending colon. The descending colon was visualized in the center of the left hemiabdomen, running to the caudal and dorsal abdomen and continuing through the pelvic canal as the rectum. Heterogeneous attenuated fecal material mixed with gas was observed predominantly in the ascending colon; however, the descending colon was also mildly distended with gas. The maximum luminal diameter of the colon observed in region of transverse and descending colon was 0.84 ± 0.25 cm.

Small foreign bodies with high attenuation (mineral) were identified in the stomach of four rabbits (17.39%), in the small intestines of one rabbit (4.34%), in the cecum of ten rabbits (43.47%) and in the colon in three rabbits (13.04%). These structures had different shapes and diameters (from 0.3 to 1.7 cm), but there were no signs of pathology associated with them.

The intrabdominal fat surrounding the abdominal organs and the serosal margins, were visualized and subjectively evaluated in all rabbits. Five rabbits (21.74%), four of which were female and one male, had more intrabdominal fat compared to the others. In these animals the serosal margins were more clearly defined, and there the intestinal segments were separated, making it easier to evaluate the walls, whether or not the organs were distended.

On the interobserver analysis the highest coefficients were in stomach length, cardia thickness, pylorus thickness, and descending colon length and thickness. All the analyzes are presented in Figure 6. The concordance or agreement between the observers was analyzed for thickness of GI tract structures, stomach height and length in sagittal plane, stomach length in dorsal plane, spinal vertebral length (L1 to coxofemoral joint). Although there were differences in results between observers the distribution and variations were still shown to be reliable.

The distention (length, height and width) of the stomach and cecum was correlated with wall thickness (see Table 6). The only parameters for which no significant correlation was identified was for gastric height and pyloric wall thickness, considering $p < 0.05$ (Graphic 3).

Table 4. Intraobserver analysis (mean and standard deviation) of CT measurements of GI tract, and dimension of the GI tract, expressed as percentages using the coefficient of variations (CV). Considering * $p < 0.05$.

	MEAN ± ST (%)	CV MINIMU M	CV MAXIMUM
Stomach distension length (cm) DP	14.38 ± 27.71	0.88	139.08
Stomach distension height (cm) TP	2.50 ± 2.84	0.16	12.20
Stomach distension width (cm) TP	5.64 ± 8.54	0.00	41.63
Stomach long axis of distension degree – length (cm) SP	8.10 ± 8.37	0.42	35.49

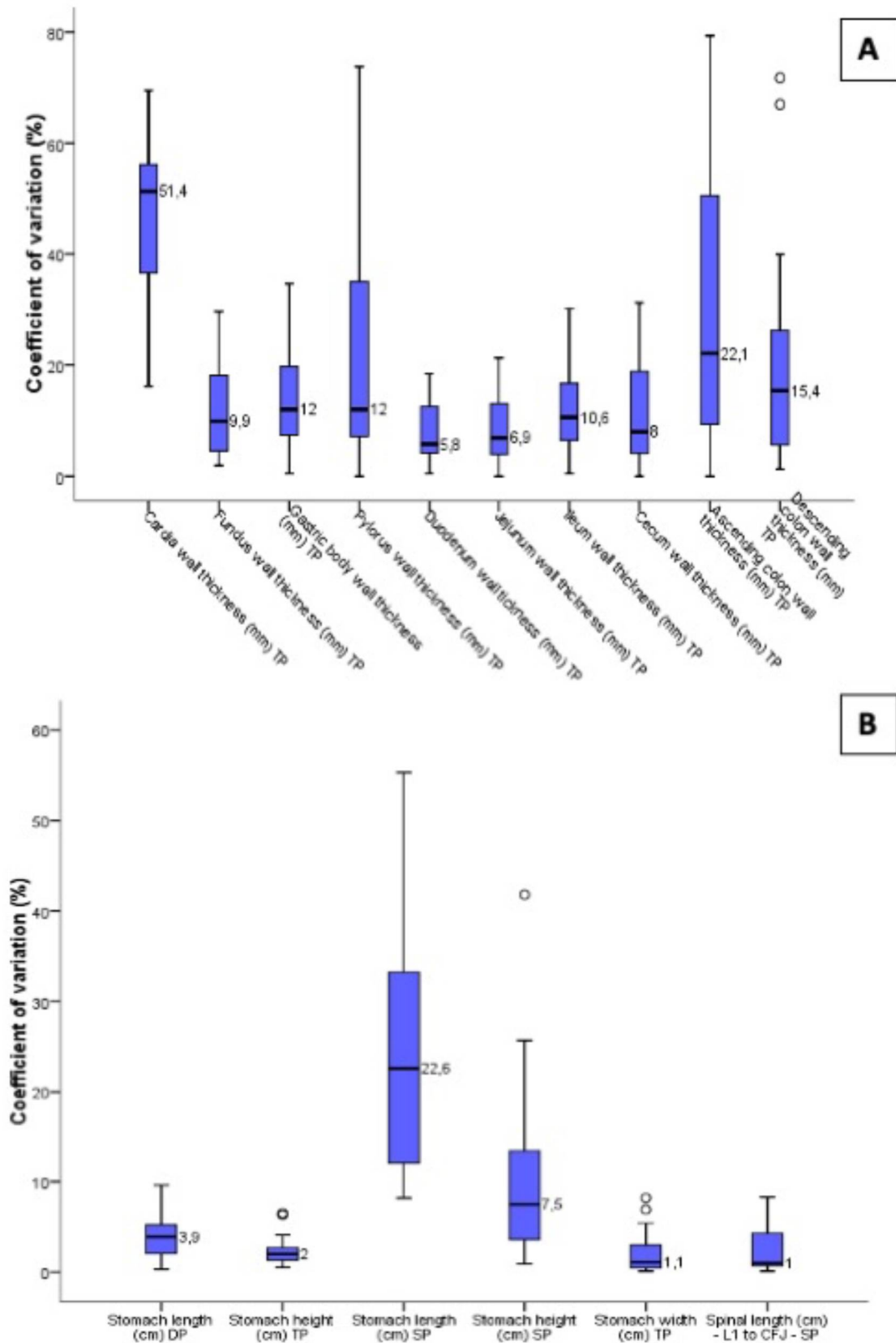
Stomach short axis distension degree – height (CM) SP	4.40 ± 4.34	0.32	17.66
Spinal length (cm) - L1 to CFJ – SP	5.03 ± 15.22	0.00	73.57
Cecum distension length (cm) DP	1.70 ± 1.50	0.13	6.72
Cecum distension width (cm) DP	8.97 ± 7.94	0.62	27.17
Cecum distension height (cm) TP	15.97 ± 19.60	0.59	83.31
Cardia wall thickness (mm) TP	9.91 ± 8.79	0.00	32.71
Fundus wall thickness (mm) TP	12.71 ± 6.73	0.52	24.82
Body wall thickness (mm) TP	13.99 ± 9.21	1.02	41.59
Pylorus wall thickness (mm) TP	10.00 ± 6.44	0.44	21.89
Duodenum wall thickness (mm) TP	13.37 ± 8.66	0.00	33.17
Jejunum wall thickness (mm) TP	8.37 ± 7.11	1.92	24.28
Ileum wall thickness (mm) TP	14.51 ± 7.04	3.52	27.39
Cecum wall thickness (mm) TP	8.22 ± 5.74	0.64	24.34
Ascending colon wall thickness (mm) TP	19.49 ± 13.20	0.00	52.06
Descending colon wall thickness (mm) TP	13.63 ± 11.34	1.85	50.57

Table 5. Quantitative analysis (mean and standard deviation) of CT measures of the distension GI tract, and wall thickness, and differences between results according to sex in first three columns, and the interobserver analysis in percentage by the coefficient of variations (CV). Considering * $p < 0.05$.

	Overall (n=23)	Females (n=14)	Males (n=9)	CV ± ST	CV MIN	CV MAX
Abdominal circumference (cm)	33.5 ± 5.2	35.6 ± 5.5 *	30.3 ± 2.5 *	NA	NA	NA
Body weight (kg)	2.8 ± 0.7	3 ± 0.8 *	2.4 ± 0.3 *	NA	NA	NA
Stomach distension length (cm) DP	4.7 ± 1.3	4.6 ± 1.4	4.8 ± 1.2	4.0 ± 2.6%	0.3%	9.6%
Stomach distension height (cm) TP	4.3 ± 0.5	4.4 ± 0.6	4.1 ± 0.4	2.4 ± 1.6%	0.5%	6.5%
Stomach distension width (cm) TP	8 ± 1.41.4	8.1 ± 1.5	7.7 ± 1.3	2.2 ± 2.3%	0.1%	8.2%
Stomach long axis distension – length (cm) SP	3.9 ± 1.2	4.1 ± 1.4	3.7 ± 0.8	24.4 ± 13.3%	8.2%	55.3%
Stomach short axis distension – height (cm) SP	4.4 ± 0.5	4.5 ± 0.5	4.3 ± 0.4	10.4 ± 9.4%	0.9%	41.8%
Cardia wall thickness (mm) TP	3.4 ± 0.4	3.4 ± 0.5 *	3.3 ± 0.3 *	47.2 ± 15%	16.2%	69.5%
Fundus wall thickness (mm) TP	1.4 ± 0.2	1.4 ± 0.2	1.4 ± 0.1	11.7 ± 8.6%	1.9%	29.6%

Body wall thickness (mm) TP	1.4 ± 0.1	1.4 ± 0.2	1.4 ± 0.1	13.4 ± 9.4%	0.5%	34.7%
Pylorus wall thickness (mm) TP	2.9 ± 0.5	2.8 ± 0.5	3.0 ± 0.5	23.8 ± 22.7%	0.0%	73.8%
Duodenum wall thickness (mm) TP	1.4 ± 0.1	1.4 ± 0.1	1.3 ± 0.1	8.0 ± 5.6%	0.5%	18.4%
Jejunum wall thickness (mm) TP	1.2 ± 0.1	1.2 ± 0.1	1.2 ± 0.1	8.6 ± 6.5%	0.0%	21.3%
Ileum wall thickness (mm) TP	1.4 ± 0.1	1.4 ± 0.1	1.3 ± 0.1	12.1 ± 8.4%	0.5%	30.2%
Cecum wall thickness (mm) TP	1.2 ± 0.1	1.2 ± 0.1	1.1 ± 0.1	11.6 ± 9.5%	0.0%	31.2%
Cecum distension length(cm) DP	11.7 ± 2.1	11.7 ± 2.2	11.5 ± 1.9	NA	NA	NA
Cecum distension width (cm) DP	9.4 ± 1.6	9.7 ± 2.0	8.9 ± 0.7	NA	NA	NA
Cecum distension height (cm) TP	2.6 ± 0.7	2.9 ± 0.7	8.9 ± 0.7	NA	NA	NA
Ascending colon wall thickness (mm) TP	1.4 ± 0.3	1.4 ± 0.2	1.6 ± 0.4	29.3 ± 24.2%	0.0%	79.4%
Descending colon wall thickness (mm) TP	1.3 ± 0.3	1.2 ± 0.1 *	1.5 ± 0.3 *	20.2 ± 19.1%	1.3%	71.8%
Spinal length (cm) - L1 to CFJ - SP	15.1 ± 1.2	15.5 ± 1.3	14.5 ± 0.9	2.7 ± 2.9%	0.1%	8.3%

TP = Transverse plane, DP = Dorsal plane , SP = Sagittal plane ,L1 = First lumbar vertebra, CFJ = Coxofemoral joint, CV = Coefficient of variation , MIN = Minimum, MAX = Maximum, NA = Not analyzed. SD= Standard deviation.



Graphic 2. Coefficient of variation boxplot of variables measured (length, height and width of cecum and stomach, and the wall thickness of GI tract) between observers expressed in percentage (estimated in mean, interquartile interval, minimum and maximum).

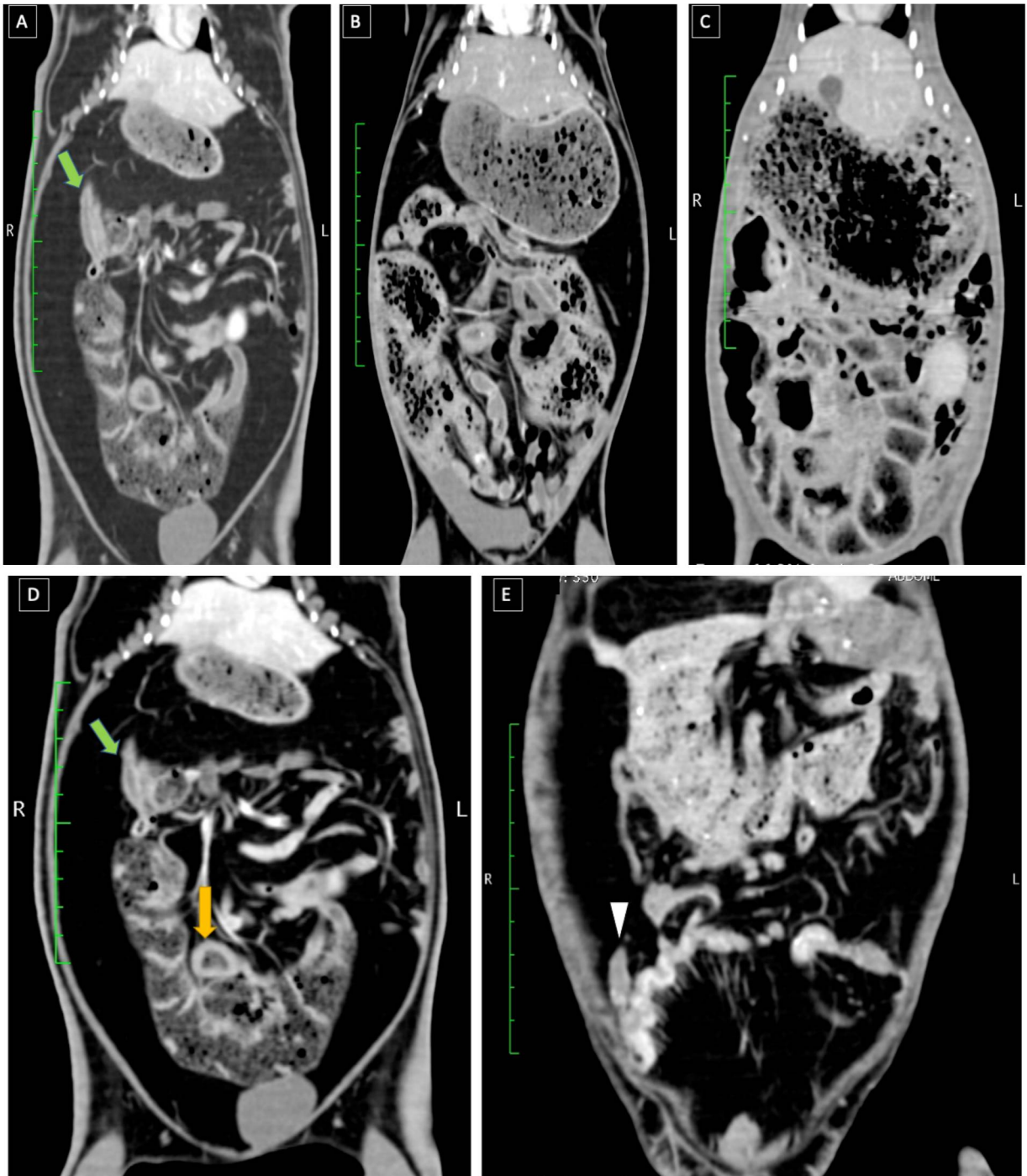
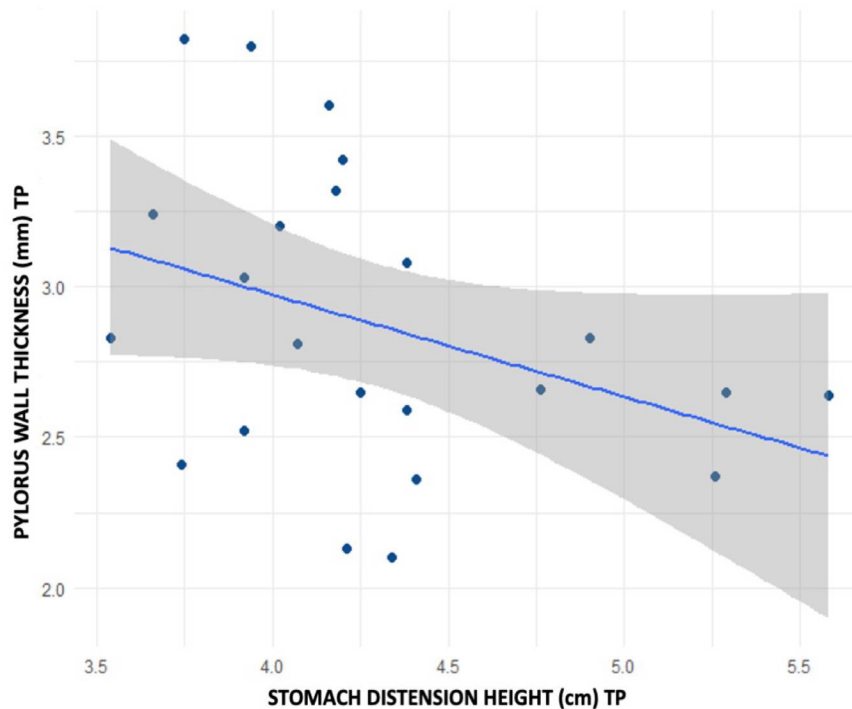


Figure 6. CT images in dorsal reconstructions of GI tract in arterial post-contrast (soft tissue window). (A) Heterogeneous content in stomach (ingesta), cecum (feces) and fluid content in duodenum (green arrow); (B) Stomach distended by heterogeneous content in stomach, in cecum the same heterogeneous material was observed, and fluid content in small intestine; (C) Distention and gas and ingesta filling stomach and cecum; (D) Location of the sacculus rotundus (yellow arrow) and distal duodenum (green arrow); (E) Location of the vermiform cecal appendix (white arrow).

Table 6. Correlation coefficient of CT measurements showing the relationship between distension of the stomach and cecum with wall thickness. Considering * $p < 0.05$.

	Cardia wall thickness (mm) TP		Fundus wall thickness (mm) TP		Body wall thickness (mm) TP		Pylorus wall thickness (mm) TP	
	CC	<i>p-value</i>	CC	<i>p-value</i>	CC	<i>p-value</i>	CC	<i>p-value</i>
Stomach distention length (cm) DP	0.104	0.634	-0.008	0.970	0.057	0.793	0.233	0.284
Stomach distention height (cm) TP	0.059	0.788	0.093	0.669	0.134	0.541	-0.414	0.048
Stomach distention width (cm) TP	0.182	0.405	0.024	0.911	0.336	0.116	0.082	0.709
Stomach long axis distention – length (cm) SP	-0.083	0.704	-0.274	0.205	0.075	0.731	0.142	0.515
Stomach short axis distention – height (cm) SP	0.008	0.969	-0.295	0.171	<0.001	0.999	-0.113	0.607

	Cecum wall thickness (mm) TP	
	CC	<i>p-value</i>
Cecum distention length (cm) DP	-0.378	0.074
Cecum distention width (cm) DP	-0.217	0.318
Cecum distention height (cm) TP	-0.101	0.645



Graphic 3. Pyloric wall thickness compared to stomach height (distention) showing that there is no correlation between the two variants. The pyloric wall thickness may remain unchanged when the stomach is distended in height. Thus, stomach length is a better parameter for assessing distension of the pylorus.

3.5 DISCUSSION

GI tract diseases are common in pet rabbits due to husbandry and feeding conditions^{5,7,17,19,21-24,27}. The common methods of imaging diagnosis have severe limitations in detecting gastric and intestinal abnormalities in rabbits, making clinical diagnosis challenging in this species^{1,8,13,26,33}. Advanced imaging modalities, such as CT, may be more effective in the anatomical evaluation of the GI system. This study presents specific tomographic reference values for the GI tract in rabbits.

The dorsal plane reformatting of the CT images allowed better definition of the degree of distension and position in the abdominal cavity and better visualization of the J or U-like shape. On the sagittal plane reformatting the gastric silhouette was ball-shaped¹. As reported in the literature, the gastric wall appears very thin on CT exams¹². The wall thickness varied according to the different regions of the stomach, the cardia and the pylorus had the thickest walls. The structure of the cardiac orifice means that rabbits cannot vomit or eructate¹², explaining the thicker walls in this region. It is important to note that no folds were

identified in the gastric mucosal surface, probably corresponding to the differences in this species' gastric physiology^{1,5,16}. Although the wall layers can be differentiated on ultrasound their density on CT is very similar and there was poor contrast between the mucosa and muscle region and the muscular layer. The fundus comprises a large part of the stomach, located in the midplane to the left side of abdomen with the pylorus to the right side as previously described⁵. The pyloro-duodenal region was visible, even when the stomach was distended with food, which suggests that CT may be very useful in examination of this common point of obstruction.

The stomach is located between the levels of T10 and T13 or L1, however in 30.43% of animals the stomach extended cranially to L2. Some studies have suggested that pathology exists if the gastric margins do not extend beyond the last rib or extend beyond L1^{8,15,23-24,34,47}, others state that the stomach may extend as far as L2 in normal animals¹. The variability in size of the normal stomach should be considered when gastric stasis or GI syndrome is suspected since significant distension is possible post-prandially. Commonly the gastric lumen is heterogeneous, mottled soft tissue opaque material and gas density on CT scans as reported in the literature as a radiographic finding^{1,5,10}. We also identified an acute angle between the pylorus and duodenum in the right abdomen^{16-17,20-25}. The liver lobe position promotes this angulation, and contrast accorded by fat in this region allows good differentiation of the margins of the abdominal organs in the cranial abdomen.

The small intestine is shorter in rabbits than other mammals^{5,8,17,20,22-25}. The segments were observed in the cranial abdomen, mostly distributed on the left side, and dorsal to the cecum. All segments of intestines could be distinguished, which is in contrast to reports of radiographic studies, in which it was not possible to distinguish small from large intestines¹. In a study analyzing intestinal obstruction in dogs we established luminal diameter to be between 0.51 and 0.65 cm⁴. The intestinal diameter/L5 height ratio in normal rabbits was 1.16 ± 0.13 but further studies are needed to investigate this in rabbits with GI disease. In our study the sacculus rotundus was identified in 47.82% of rabbits, however literature reports suggest that the sacculus rotundus is visible on both US and CT exams due to the abundant lymphoid tissue found there^{3,18,21,22,25,28}. Due to the difficulty in routinely locating this structure in our study, wall measurements were

not taken. However, a previous study detected abnormalities in wall thickness of the sacculus rotundus on ultrasonography (0.8 cm) and CT (0.77 cm)²⁵. The normal GI tract conditions and degree of distension of the large intestine can compress the sacculus rotundus explaining the difficulties in identifying and determining the wall thickness of this structure.

The cecal features described in the literature were visible on CT^{17,18,25,26}. It has been reported that the cecum extends from the level of L1 to L6¹, however we found the cranial margin of the cecum most commonly at the level of T12 and T13, and the caudal margin at the sacral region or L7 demonstrating the variation in size of this organ under normal conditions, mainly due to gas distention. As for the sacculus rotundus, the appendix was identified in only 43.48% of rabbits, and because of this limited visualization wall measurements were not made. If the GI tract was more distended by gas and/or ingesta there was more compression and displacement of the sacculus rotundus and appendix, making anatomical evaluation difficult. For animals that had emptier intestines and more abdominal fat, the anatomical positions were maintained, and identification of structures was easier. Other researchers have previously reported reference values for appendix wall thickness in rabbits^{25,31}.

The proximal and distal part of the colon was identified, and the fusus coli did not distinguished in this study. The distal colon usually containing hard fecal pellets^{3,5,19-24,26-27}. The mean luminal diameter of the colon was 5.9-19.00 mm, and a radiographic study determined the maximum diameter to be in 6.44–18.35 mm¹. The similarity of these findings gives confidence in the normal values for diameter of the large intestine.

There were significant statistical differences between descending colon wall thickness between sexes. The colon in females is less distended because the uterus and vagina occupy space in this region. In our study 71.4% of females were sexually intact which may explain our finding of thicker colon wall in this sex.

Foreign bodies were seen in 18 animals, mostly in the cecum, which were not seen on the US exam performed before CT. Although there was variation in the size and shape of foreign bodies, there was no evidence of obstruction or any GI wall damage. According to the literature, the proximal duodenum and terminal portion of the ileum are the common sites of obstruction due to luminal narrowing in these areas^{8,12}.

The intraobserver disagreement was observed indicates that although the observer knows the correct measurement region for the different portions of the GI tract, the differences observed between measurements show that due to the thin wall thickness and also the poor interface delimiting the mucosa and serosa, repeatability is more difficult. The disagreement between observers may be explained mainly by the same reasons of intraobserver analysis, despite de experience between observers. But other reasons should be considered, including the difficulty in delimiting the walls of the cardia, because there is little external contrast around this region. The degree of gastric distention also affected accurate cardia wall delimitation. Another possible causes of interobserver variation, particularly for assessment of gastric and colonic wall thickness, was that the same slice was not chosen by each observer for measurement (Figure 3). It is suggested standardizing wall measurements in rabbits by inflation of the colon with fluid or gas⁴³.

There was a strong correlation between stomach length and the wall thickness of the fundus and body of the stomach, ie. in animals with less gas or ingesta within the stomach the wall was thicker. This meant that the wall was easier to identify, and measurements could be performed more easily. However, there was a weak correlation between stomach length and pyloric wall thickness, which was instead correlated with stomach width and no correlation between stomach height and pyloric wall thickness. Thus, stomach length is a better parameter for assessing distension and correlate to the pylorus wall. This variable correlation between parameters suggests that the parameters of length, width and height should be evaluated together to interpret the degree of gastric distension.

The cecal wall is thinner than that of many of the other intestinal tract segments. Cecal wall thickness was less affected by the degree of distension than the stomach wall.

This study has a number of limitations including the small sample size which made it difficult to analyze breed variations and the variations between males and females. CT is a superior modality for analysis of many parameters compared with abdominal ultrasonography and radiography, since the gastrointestinal physiology and anatomy of rabbits does not interfere with image formation. However, the degree of intestinal distension can make identification of

some important regions, such as the sacculus rotundus and the appendix, difficult. The technical limitations of CT also hamper assessment of GI wall layering, and differentiation of the layers is much better seen with US. Another limitation was the small number, and difference in experience, of the observers, although we show that it is possible to evaluate the GI structures despite the observer disagreements. Although sedation or general anesthesia is usually required to minimize motion artefact and allow detailed assessment of images, conscious CT using a VetMousetrap™ device, may give valuable information in an emergency^{25,48-52}.

CT evaluation of the gastrointestinal tract provided more detail compared to traditional imaging techniques in rabbits. However, the degree of gastric and cecal distension may interfere with measurements of wall thickness of gastrointestinal tract structures, in identification and assessment of cecal structures (sacculus rotundus and appendix).

3.6 CONCLUSION

In summary, routine CT of rabbits can allow assessment of the entire GI tract, acquisition of measurements, anatomical correlations, and the severity of distention (with gas or ingesta). The rabbit stomach is large, thin walled, and always contains some ingesta and gas. The sacculus rotundus is an enlarged sac-like structure located at the terminal portion of the ileum although the associated lymphoid tissue may not identify in some CT images. The cecum, which is the most important part of the digestive system in rabbits, is a blind sac that is the most prominent organ in the abdomen and has a capacity 10 times that of the stomach. The vermiform cecal appendix is the terminal part of cecum and is characteristic of rabbits but is not visible in some CT images when there is more intestinal distention.

3.7 ACKNOWLEDGEMENTS

Our sincere thanks go to the owners who agreed to collaborate with this study, to the residents responsible for the cases, to the coordination for the improvement of higher-level personnel (CAPES), to the Bionostic imaging diagnostic center

which encourages scientific research and collaborated and made available the computed tomography service. And finally, to Camila Marinelli Martins for her statistical consultancy.

3.8 REFERENCES

1. Balikçi Dorotea S, Banzato T, Bellini L, Contiero B & Zotti A. Radiographic anatomy of dwarf rabbit abdomen with normal measurements. *Bulg. J. Vet. Med.*, 2016; 19 (2), 96–107.
2. Mäkitaipale J, Harcourt-Brown FM, Laitinen-Vapaavuori O. Health survey of 167 pet rabbits (*Oryctolagus cuniculus*) in Finland. *Vet Record*. 2015. 177(16), 418. doi:10.1136/vr.103213.
3. Stan F, Damian A, Gudea A, Dezdrobotu C, Bob D, Martonoş C, Bochis I, Pogana B. Comparative Anatomical Study of the Large Intestine in Rabbit and Chinchilla. *Bulletin UASVM Veterinary Medicine*. 2014; 71(1) 208-212.
4. Mackey EB, Hernandez-Divers SJ, Holland M, Frank P. Clinical Technique: Application of computed tomography in zoological medicine. *J. Exotic Pet Med*. 2008; 17 198-209.
5. Nath SK, Das S, Kar J, Afrin K, Dash AK, Akter S. Topographical and biometrical anatomy of the digestive tract of White New Zealand Rabbit (*Oryctolagus cuniculus*). *Journal of Advanced Veterinary and Animal Research*. 2016; 3(2): 145-151.
6. Naff KA, Craig S. The Domestic Rabbit, *Oryctolagus Cuniculus*: Origins and History. In: *The Laboratory Rabbit, Guinea Pig, Hamster, and Other Rodents*. Suckow M, Stevens K, Wilson R. United Kingdom: Elsevier Ltda. 1st ed, 2012. 6 157-163.
7. Donnelly TM, Vella D. Basic Anatomy, Physiology, and Husbandry of Rabbits. In: *In: Ferrets, Rabbits and Rodents Clinical Medicine and Surgery*, Quesenberry KE, Orcutt CJ, Mans C, Carpenter JW . St Louis, MO, Saunders. 4th ed., 2020, 11 135-136.
8. Debenham JJ, Brinchmann T, Sheen J, Vella D. Radiographic diagnosis of small intestinal obstruction in pet rabbits (*Oryctolagus cuniculus*): 63 cases. *Journal of Small Animal Practice*. 2019; 60(11), 1-6.
9. Oparil KM, Gladden JN, Babyak JM, Lambert C, Graham JE. Clinical characteristics and short-term outcomes for rabbits with signs of gastrointestinal tract dysfunction: 117 cases (2014–2016) *Journal of the American Veterinary Medical Association JAVMA*, 2019, 255 (7), 837-845.
10. DeCubellis J. Common Emergencies in Rabbits, Guinea Pigs, and Chinchillas. *Vet Clin Exot Anim*. 2016; 19(2), 411-429. <https://doi.org/10.1016/j.cvex.2016.01.003>.

11. Reavill D. Pathology of the exotic companion mammal gastrointestinal system. *Vet Clin North Am Exot Anim Pract.* 2014; 17(2):145-64. doi: 10.1016/j.cvex.2014.01.002.
12. Schuhmann B, Cope I. Medical treatment of 145 cases of gastric dilatation in rabbits. *Veterinary Record.* 2014; 175(19), 484. doi:10.1136/vr.102491.
13. Ritzman TK. Diagnosis and clinical management of gastrointestinal conditions in exotic companion mammals (rabbits, guinea pigs, and chinchillas) *Clin North Am Exot Anim Pract.* 2014;17(2):179-94. doi:10.1016/j.cvex.2014.01.003.
14. DeCubellis J, Graham J, Gastrointestinal Disease in Guinea Pigs and Rabbits. *Vet Clin North Am Exot Anim Pract.* 2013; 16(2): 421–435. doi: 10.1016/j.cvex.2013.01.002.
15. Preeble J. Gastrointestinal stasis and obstructive ileus in the rabbit. *The Veterinary Nurse.* 2012; 3(6): 366-372.
16. Maksimović A, Spahija N, Čamo D, Lutvikadić I. A unique case of spontaneous intestinal volvulus in a pet rabbit - Case report. *Veterinaria.* 2020, 69(1), 65-68.
17. Kohles M. Gastrointestinal anatomy and physiology of select exotic companion mammals. *Clin North Am Exot Anim Pract.* 2014;17(2):165-78. doi:10.1016/j.cvex.2014.01.010.
18. Stan F. Anatomical Particularities of the Cecum in Rabbits and Chinchillas. *Bulletin of University of Agricultural Sciences and Veterinary Medicine Cluj-Napoca. Veterinary Medicine.* 2014; 71(2). doi:10.15835/buasvmcn-vm:10587.
19. O'Malley B. Rabbits. In: *Clinical Anatomy and Physiology of Exotic Species: Structure and Function of Mammals, Birds, Reptiles and Amphibians.* United Kingdom: Elsevier Ltda. 2005; 8 173,179-187.
20. Stan F., Comparative study of the stomach morphology in rabbit and chinchilla, *AgroLife Scientific Journal.* 2013, 2(2), 73-78.
21. Donnelly TM, Vella D. Basic Anatomy, Physiology, and Husbandry of Rabbits. In: *In: Ferrets, Rabbits and Rodents Clinical Medicine and Surgery,* Quesenberry KE, Orcutt CJ, Mans C, Carpenter JW . St Louis, MO, Saunders. 4th ed., 2020, 11 135-136.
22. Meredith A. Biology, anatomy and physiology. In: *BSAVA Manual of Rabbit Medicine* Meredith A and Lord B eds. Quedgeley, Gloucester: BSAVA, 2014. 1 1-12.
23. Harcourt-Brown F. Digestive system disease. In: *BSAVA Manual of Rabbit Medicine* Meredith A and Lord B eds. Quedgeley, Gloucester: BSAVA, 2014. 12 168-190.
24. Varga M. Digestive disorders. In: *Textbook of Rabbit Medicine.* United Kingdom: Elsevier Ltda. 2nd ed. 2014, 8 303-347.
25. Longo M, Thierry F, Eatwll K, Schwarz T, Del Pozo J, Richardson J. *Vet Radiol Ultrasound.* 2018;59(5):56-60. doi: 10.1111/vru.12602.

26. Guzman, DS-M., Graham, JE, Keller, K, Hunt, G, Tong, N, & Morrissey, JK. Colonic Obstruction Following Ovariohysterectomy in Rabbits: 3 Cases. *Journal of Exotic Pet Medicine*. 2015; 24(1), 112–119. doi:10.1053/j.jepm.2014.11.006.
27. Sohn J, Couto MA. Anatomy, Physiology, and Behavior. In: *The Laboratory Rabbit, Guinea Pig, Hamster, and Other Rodents*. Suckow M, Stevens K, Wilson R. United Kingdom: Elsevier Ltda. 1st ed, 2012 8 195, 200-202.
28. Banzato T, Bellini L, Contiero B, Selleri P, Zotti A. Abdominal ultrasound features and reference values in 21 healthy rabbits. *Veterinary Record*. 2014; 176(4), 101–101. doi:10.1136/vr.102657
29. Reese S. Introduction and Sonoanatomy of gastrointestinal tract. In: *Diagnostic Imaging of Exotic Pets: Birds, Small Mammals, Reptiles*. Eds M. E. Krautwald-Junghanns, M. Pees, S. Reese, T. Tully. Schluetersche Verlagsgesellschaft mbH & Co. KG. 2010, 2 143,224-226.
30. Oura, TJ, Graham, JE, Knafo, SE, Aarsvold, S, Gladden, JN, Barton, BA. Evaluation of gastrointestinal activity in healthy rabbits by means of duplex Doppler ultrasonography. *American Journal of Veterinary Research*. 2019; 80(7), 657–662. doi:10.2460/ajvr.80.7.657
31. Nicoletti A, Di Girolamo N, Zeyen U, Selleri P, Masi M, Fonti P. Ultrasound morphology of cecal appendix in pet rabbits. *Journal of Ultrasound*. 2018. doi:10.1007/s40477-018-0316-3 .
32. Da Silva, KG, de Andrade, C, Sotomaior, CS. Influence of simethicone and fasting on the quality of abdominal ultrasonography in New Zealand White rabbits. *Acta Veterinaria Scandinavica*. 2017; 59(1). doi:10.1186/s13028-017-0316-x
33. Di Giuseppe M, Faraci L, Luparello M, Morici M, Dorrestein GM, Spadola F. Omental Torsion in a Rabbit (*Oryctolagus cuniculus*). *Journal of Exotic Pet Medicine*. 2016;25(2), 163-167.
34. Reese S, Hein J. Radioanatomy of gastrointestinal tract. In: *Diagnostic Imaging of Exotic Pets: Birds, Small Mammals, Reptiles*. Eds M. E. Krautwald-Junghanns, M. Pees, S. Reese, T. Tully. Schluetersche Verlagsgesellschaft mbH & Co. KG. 2010, 2 176-180.
35. Schwarz T, O'Brien, R: Acquisition Principles. In: *Veterinary computed tomography*. Eds Schwarz T, Saunders J. Ed 1, Oxford, Wiley-Blackwell. 2011; 2, 9-27.
36. Fehr M. Computed tomography (CT) and magnetic resonance imaging (MRI). In: *Diagnostic Imaging of Exotic Pets: Birds, Small Mammals, Reptiles*. Eds M. E. Krautwald-Junghanns, M. Pees, S. Reese, T. Tully. Schluetersche Verlagsgesellschaft mbH & Co. KG. 2010, 2 242.

37. Ghoshal, NG, Bal HS. Comparative morphology of the stomach of some laboratory animals. *Laboratory Animals*. 1989. 23, 21–29.
38. Khaleel EM, Ghafi HD. Anatomical and histological study of stomach in adult local rabbits *Oryctolagus cuniculus*. *Al-Mustansiriyah J. Sci.* 2012. 23 (7), 1-22.
39. Fitzgerald, E, Lam R, Drees R. Improving conspicuity of the canine gastrointestinal wall using dual phase contrast-enhanced computed tomography: a retrospective cross-sectional study. *Veterinary Radiology & Ultrasound*. 2017, 58(2), 151–162. doi:10.1111/vru.12467.
40. Hoey S, Drees, R, Hetzel, S. Evaluation of the gastrointestinal tract in dogs using computed tomography. *Veterinary Radiology & Ultrasound*. 2012, 54(1), 25–30. doi:10.1111/j.1740-8261.2012.01969.x.
41. Minitier BM, Gonçalves Arruda A, Zuckerman J, Caceres AV, Ben Amotz, R. Use of computed tomography (CT) for the diagnosis of mechanical gastrointestinal obstruction in canines and felines. *PLOS ONE*. 2019, 14(8), e0219748. doi:10.1371/journal.pone.0219748.
42. Kim C, Lee S-K, Je H, Jang Y, Jung J-W, & Choi J. Assessment of a split-bolus computed tomographic enterography technique for simultaneous evaluation of the intestinal wall and mesenteric vasculature of dogs. *American Journal of Veterinary Research*. 2020; 81(2), 122–130. doi:10.2460/ajvr.81.2.122.
43. Cheon B, Moon S, Park S, Lee S, Hong S, Cho H & Choi J. Comparison of contrast media for visualization of the colon of healthy dogs during computed tomography and ultrasonography. *American Journal of Veterinary Research*. 2016; 77(11), 1220–1226. doi:10.2460/ajvr.77.11.1220.
44. Drost, W. T., Green, E. M., Zekas, L. J., Aarnes, T. K., Su, L., & Habing, G. G. Comparison of computed tomography and abdominal radiography for detection of canine mechanical intestinal obstruction. *Veterinary Radiology & Ultrasound*. 2016; 57(4), 366–375. doi:10.1111/vru.12353.
45. Winter, M. D., Barry, K. S., Johnson, M. D., Berry, C. R., & Case, J. B. Ultrasonographic and computed tomographic characterization and localization of suspected mechanical gastrointestinal obstruction in dogs. *Journal of the American Veterinary Medical Association*. 2017; 251(3), 315–321. doi:10.2460/javma.251.3.315.
46. Veraa S & Schoemaker N. CT and MRI scanning and interpretation. In: *Manual of Rabbit Surgery, Dentistry and Imaging*. Harcourt-Brown F, Chitty J. Quedgeley, Gloucester: BSAVA, 2014. 9. 107-114.
47. Lichtenberger, M., & Lennox, A. Updates and Advanced Therapies for Gastrointestinal Stasis in Rabbits. *Veterinary Clinics of North America: Exotic Animal Practice*, 13(3), 525–541, 2010. doi:10.1016/j.cvex.2010.05.008
48. Shanaman, M. M., Hartman, S. K., & O'Brien, R. T. Feasibility for using dual-phase contrast-enhanced multi-detector helical computed

- tomography to evaluate awake and sedated dogs with acute abdominal signs. *Veterinary Radiology & Ultrasound*. 2012; 53(6), 605–612. doi:10.1111/j.1740-8261.2012.01973.x
49. Shanaman, M. M., Schwarz, T., Gal, A., & O'Brien, R. T. Comparison Between Survey Radiography, B-Mode Ultrasonography, Contrast-Enhanced Ultrasonography and Contrast-Enhanced Multi-Detector Computed Tomography Findings in Dogs with Acute Abdominal Signs. *Veterinary Radiology & Ultrasound*. 54 (6), 591–604, 2013. doi:10.1111/vru.12079.
50. Oliveira, C. R., Ranallo F. N., Pijanowski G. J., Mitchell, M. A., O'brien M. A., Mcmichael M., Shartman S.K., Matheson J. S., O'brien, R. T. *The Vetmousetrap™: A Device for computed tomographic imaging of the thorax of awake cats*. *Veterinary Radiology & Ultrasound*, 52(1), 41–52, 2011. doi:10.1111/j.1740-8261.2010.01726.x.
51. Oliveira, C. R., Mitchell, M. A., & O'Brien, R. T. Thoracic computed tomography in feline patients without use of chemical restraint. *Veterinary Radiology & Ultrasound*, 52(4), 368–376, 2011. doi:10.1111/j.1740-8261.2011.01814.x
52. Dozeman, E.T., Prittie, J.E., Fischetti, A.J. Utilization of the vetmouse trap for whole body computed tomography in polytrauma patients (S36). The Animal Medical Center, New York, NY. In Abstracts from the International Veterinary Emergency and Critical Care Symposium, the European Veterinary Emergency and Critical Care Annual Congress, and the ACVECC VetCOT Veterinary Trauma & Critical Care Conference 2018. *Journal of Veterinary Emergency and Critical Care*, 28(S1), S1–S37, 2018. doi:10.1111/vec.12758.

4. FINAL CONCLUSIONS

Radiographic and ultrasonographic examinations are commonly used for evaluation of the gastrointestinal tract of pet rabbits. CT has a number of advantages over these modalities and allows a detailed evaluation of the abdominal structures of rabbits. In this study we report reference values for kidney, ureter, urinary bladder, stomach and intestinal (small and large) size in rabbits.

Veterinarians would get value from the use of CT to complement clinical examination. As advanced diagnostic imaging modalities become more accessible, radiologists will be increasingly asked to evaluate images from exotic pets. Therefore, it is necessary to acquire specific knowledge of the anatomy and physiology of these small pets, especially rabbits, to provide accurate interpretation of CT images, contributing to faster and accurate diagnoses.

REFERENCES

PET FOOD MANUFACTURES ASSOCIATION (PMFA). **Pet population**. 2020. Available in: <<https://www.pfma.org.uk/pet-population-2020>>. Access on January 30, 2021.

AMERICAN VETERINARY MEDICAL ASSOCIATION (AVMA). **U.S. Pet ownership statistics**. 2017-2018. Available in: <<https://www.avma.org/resources-tools/reports-statistics/us-pet-ownership-statistics>>. Access on January 30, 2021.

ASSOCIAÇÃO BRASILEIRA DA INDÚSTRIA DE PRODUTOS PARA ANIMAIS DE ESTIMAÇÃO (ABINPET). **MERCADO PET BRASIL**. 2019. Disponível em: <<http://abinpet.org.br/mercado/>>. Acesso em 30 de janeiro de 2021.

DONNELLY, T.M.; VELLA, D. Basic Anatomy, Physiology, and Husbandry of Rabbits. In: QUESENBERRY KE, ORCUTT CJ, MANS C, CARPENTER JW. **Ferrets, Rabbits and Rodents Clinical Medicine and Surgery**. St Louis, MO, Saunders. 4th ed., 11, p.135-136, 2020.

NAFF, K. A.; CRAIG, S. The Domestic Rabbit, *Oryctolagus Cuniculus*: Origins and History In: SUCKOW, M. A.; STEVENS, K. A.; WILSON, R. P. **The Laboratory Rabbit, Guinea Pig, Hamster, and Other Rodents**, St. Louis, Elsevier, p.157-163, 2012.

MARTIN, B. J. Taxonomy and History In: SUCKOW, M. A.; STEVENS, K. A.; WILSON, R. P. **The Laboratory Rabbit, Guinea Pig, Hamster, and Other Rodents**, St. Louis, Elsevier, p. 949-953, 2012.

SOHN, J.; COUTO, M. A. Anatomy, Physiology, and Behavior In: SUCKOW, M. A.; STEVENS, K. A.; WILSON, R. P. **The Laboratory Rabbit, Guinea Pig, Hamster, and Other Rodents**, St. Louis, Elsevier, p.195-215, 2012.

O'MALLEY B. Rabbits. In: **Clinical Anatomy and Physiology of Exotic Species: Structure and Function of Mammals, Birds, Reptiles and Amphibians**. United Kingdom: Elsevier Ltda. 8, p. 173,179-187, 2005.

PESSOA C. A. Lagomorpha (Coelho, Lebre e Tapiti). In: CUBAS Z. S.; SILVA J.C.; CATÃO-DIAS J.L. **Tratado de animais selvagens – Medicina Veterinária**. 2ª ed., São Paulo, Roca, vol 2., 56. p. 2526-2578, 2015.

SCHWARZ, T.; O'BRIEN, R. **Acquisition Principles**. In: SCHWARZ T.; SAUNDERS J., **Veterinary computed tomography**. 1st ed., Oxford, Wiley-Blackwell, 2, p.9-27, 2011.

DREES, R. Rabbits and Rodents. In: SCHWARZ T, SAUNDERS J. **Veterinary computed tomography**. 1st ed., Oxford, Wiley-Blackwell. 48, 509-516, 2011.

FEHR M. Computed tomography (CT) and magnetic resonance imaging (MRI). In: M.E. Krautwald-Junghanns, M. Pees, S. Reese, T. Tully. **Diagnostic Imaging of Exotic Pets: Birds, Small Mammals, Reptiles**. Schluetersche Verlagsgesellschaft mbH & Co. KG. p.242-243, 2010.

OHLERTH S.; SCHARF G. **Computed tomography in small animals – Basic principles and state of the art applications**. The Veterinary Journal, 173 (2), p. 254–271, 2007. <https://doi.org/10.1016/j.tvjl.2005.12.014>.

DILEK, O.G.; DIMITROV, R.; STAMATOVA-YOVICHEVA, K. **The role of imaging anatomy in the contemporary anatomical studies of domestic rabbits in veterinary and agricultural science**. Bulgarian Journal of Agricultural Science, 25 (3), p. 575–580, 2019.

MACKEY, E. B.; HERNANDEZ-DIVERS, S. J.; HOLLAND, M. & FRANK, P. **Clinical Technique: Application of computed tomography in zoological medicine**. J. Exotic Pet Med., 17, p.198-209, 2008.

VAN-ZEELAND, Y. **Rabbit Oncology. Veterinary Clinics of North America: Exotic Animal Practice.** 20(1), 135–182. 2017. doi:10.1016/j.cvex.2016.07.005.

KIM, R.; KIM, S.Y.; CHO, J.Y.; LEE, J.; KIM, S.H. **Use of Iterative Reconstruction and a Small Contrast Volume in Rabbit Kidney CT: Comparison with Conventional Protocol.** J Korean Soc Radiol. 2018, 79(2), p.77-87. <https://doi.org/10.3348/jksr.2018.79.2.77>.

VILALTA, L.; ALTUZARRA, R.; ESPADA, Y.; DOMINGUEZ, E.; NOVELLAS. R.; MARTORELL, J. **Description and comparison of excretory urography performed during radiography and computed tomography for evaluation of the urinary system in healthy New Zealand White rabbits (*Oryctolagus cuniculus*).** American Journal of Veterinary Research. 78(4), p. 472–481, 2017. doi:10.2460/ajvr.78.4.472.

ZOLLER, G., LANGLOIS, I., ALEXANDER, K. **Glomerular filtration rate determination by computed tomography in two pet rabbits with renal disease.** Journal of the American Veterinary Medical Association, 250(6), p.681–687, 2017. doi:10.2460/javma.250.6.681.

KAYA, M.; BUMIN, A.; SEN, Y.; AALKAN, Z. **Comparison of Excretory Urography, Ultrasonography-Guided Percutaneous Antegrade Pyelography, and Renal Doppler Ultrasonography in Rabbits with Unilateral Partial Ureteral Obstruction: An Experimental Study.** Kafkas Univ Vet Fak Derg. 6(5), p.735-741, 2010. doi:10.9775/kvfd.2009.1557.

EKEN, E.; ÇORUMLUOĞLU, Ö.; PAKSOY, Y.; BESOLUK, K.; KALAYCI, İ. **A study on evaluation of 3D virtual rabbit kidney models by multidetector computed tomography images.** Anatomy. Anatomy, 3, p.40-44, 2009. doi:10.2399/ana.09.009.

YONKOVA, P.; DIMITROV R., TONEVA, J.; ZAPRJANOVA, D. **A Comparative study of cross-sectional anatomy and computed tomography of perirenal fat depots in New Zealand White rabbits.** Trakia J. Sci., 8, p.74–78, 2010.

SNIPES, R. L., CLAUSS, W., WEBER, A., & HORNICKE, H. **Structural and functional differences in various divisions of the rabbit colon.** Cell and Tissue Research, 225(2), 1982. doi:10.1007/bf00214686

LONGO, M.; THIERRY, F.; EATWLL, K.; SCHWARZ, T.; DEL POZO, J.; RICHARSON, J. **Ultrasound and computed tomography of sacculitis and appendicitis in a rabbit.** Vet Radiol Ultrasound. 59(5), p. 56-60, 2018. doi: 10.1111/vru.12602.

DAGGETT, A.; LOEBER, S.; LE ROUX, A. B.; BEAUFRERE, H.; DOSS, G. **Computed tomography with Hounsfield unit assessment is useful in the diagnosis of liver lobe torsion in pet rabbits (*Oryctolagus cuniculus*).** Vet Radiol Ultrasound. p.1-8, 2020. doi:10.1111/vru.12939.

STAMATOVA-YOVICHEVA, K.; DIMITROV, R.; YONKOVA, P.; RUSSENOV, A.; YOVICHEV, D.; KOSTOV, D. **Comparative Imaging Anatomic Study of Domestic Rabbit Liver (*Oryctolagus Cuniculus*).** Trakia Journal of Sciences, vol.10, 1, p. 57-63, 2012.

STAMATOVA-YOVICHEVA, K.; DIMITROV R.; TONEVA Y.; YONKOVA P.; KOSTOV D.; RUSENOV A.; UZUNOVA K.; YORDANOVA, V. **Helical computed tomography application in rabbit liver anatomy: comparison with frozen cross-sectional cuts.** Turkish Journal of Veterinary Animal Sciences. 37, p. 553–558. 2013. doi:10.3906/vet-1211-6.

KAWATA, R.; SAKATA, K.; KUNIEDA, T.; SAJI, S.; DOI, H. & NOZAWA, Y. **Quantitative evaluation of fatty liver by computed tomography in rabbits.** *American Journal of Roentgenology*, 142 (4), p. 741–746, 1984 doi:10.2214/ajr.142.4.741.

DIMITROV, R. S. **Computed tomography imaging of the prostate gland in the rabbit (*Oryctolagus cuniculus*)**. Veterinarski Arhiv, 80 (6), p.771-778, 2010.

DIMITROV, R.; YONKOVA, P. & STAMATOVA-YOVICHEVA, K. **Agreement Between Sagittal Plane Cross Sectional Anatomy, Sonoanatomy And Computed Tomography of Rabbit Prostate and Bulbourethral Glands**. Bulgarian Journal of Veterinary Medicine, 14, 1, p.11–16, 2011.

DIMITROV, R. **Anatomical Imaging Analysis of the Prostate gland in Rabbit (*Oryctolagus cuniculus*) - Helical computed tomography study**. Revue Méd. Vét.,164, 5, p. 245-25, 2013.

ZEHNDER, A. M.; HAWKINS, M. G.; TRESTRAIL, E. A.; HOLT, R. W. & KENT, M. S. **Calculation of body surface area via computed tomography–guided modeling in domestic rabbits (*Oryctolagus cuniculus*)**. American Journal of Veterinary Research, 73 (12), p.1859-1863, 2012. doi:10.2460/ajvr.73.12.1859

ITOH, T.;KAWABE, M.; NAGASE, T.; KOIKE, T.; MIYOSHI, M. & MIYAHARA, K. **Measurements of body surface area and volume in laboratory rabbits (New Zealand White rabbits) using a computed tomography scanner**. Experimental Animals, 67(4), p. 527–534, 2018. doi:10.1538/expanim.18-0028.

APPENDIX



UNIVERSIDADE FEDERAL DO PARANÁ
SETOR DE CIÊNCIAS AGRÁRIAS
COMISSÃO DE ÉTICA NO USO DE ANIMAIS

CERTIFICADO

Certificamos que o protocolo número 047/2019, referente ao projeto “**Estudo anatômico das estruturas abdominais, torácicas e vertebrais pela técnica de tomografia computadorizada em coelhos (*Oryctolagus cuniculus*)**”, sob a responsabilidade **Tilde Rodrigues Froes** – que envolve a produção, manutenção e/ou utilização de animais pertencentes ao filo Chordata, subfilo Vertebrata (exceto o homem), para fins de pesquisa científica ou ensino – encontra-se de acordo com os preceitos da Lei nº 11.794, de 8 de Outubro, de 2008, do Decreto nº 6.899, de 15 de julho de 2009, e com as normas editadas pelo Conselho Nacional de Controle da Experimentação Animal (CONCEA), e foi aprovado pela COMISSÃO DE ÉTICA NO USO DE ANIMAIS (CEUA) DO SETOR DE CIÊNCIAS AGRÁRIAS DA UNIVERSIDADE FEDERAL DO PARANÁ - BRASIL, com grau 1 de invasividade, em reunião de 04/09/2019.

Vigência do projeto	Outubro/2019 até Março/2021
Espécie/Linhagem	<i>Oryctolagus cuniculus</i> (lagomorfo)
Número de animais	25
Peso/Idade	3 – 5 Kg/1 – 6 anos
Sexo	Macho e fêmea
Origem	Sob tutela particular (Pacientes de Rotina do Hospital Veterinário UFPR)

CERTIFICATE

We certify that the protocol number 047/2019, regarding the project “**Anatomical study of abdominal, toracic and vertebral structures through the computed tomography in rabbits (*Oryctolagus cuniculus*)**” under **Tilde Rodrigues Froes** supervision – which includes the production, maintenance and/or utilization of animals from Chordata phylum, Vertebrata subphylum (except Humans), for scientific or teaching purposes – is in accordance with the precepts of Law nº 11.794, of 8 October, 2008, of Decree nº 6.899, of 15 July, 2009, and with the edited rules from Conselho Nacional de Controle da Experimentação Animal (CONCEA), and it was approved by the ANIMAL USE ETHICS COMMITTEE OF THE AGRICULTURAL SCIENCES CAMPUS OF THE UNIVERSIDADE FEDERAL DO PARANÁ (Federal University of the State of Paraná, Brazil), with degree 1 of invasiveness, in session of 04/09/2019.

Duration of the project	October/2019 until March/2021
Specie/Line	<i>Oryctolagus cuniculus</i> (lagomorpha)
Number of animals	25
Weight/Age	3 – 5 Kg/1 – 6 years
Sex	Male and female
Origin	Under particular guardianship (Veterinary Hospital Routine Patients – UFPR)

Curitiba, 04 de setembro de 2019

Chayane da Rocha

Chayane da Rocha

Coordenadora CEUA-SCA



UNIVERSIDADE FEDERAL DO PARANÁ
SETOR DE CIÊNCIAS AGRÁRIAS
COMISSÃO DE ÉTICA NO USO DE ANIMAIS

ANEXO 1 – TERMO DE CONSENTIMENTO LIVRE E ESCLARECIDO

O Sr(Sra.) está sendo convidado(a) a autorizar a participação de seu(s) animal(is) para fins didáticos no projeto **“Estudo anatômico das estruturas abominais, torácicas e vertebrais pela técnica de tomografia computadorizada em coelhos (*Oryctolagus cuniculus*)”** da Universidade Federal do Paraná (UFPR). Ao assinar este termo, o(a) Sr. (Sra.) permitirá que sejam realizados exames de imagem – tomografia computadorizada. Para o procedimento é necessária a **anestesia** do animal e aplicação de contraste intravenoso, sem causar dor aos animais. Os procedimentos adotados obedecem aos princípios éticos no uso de animais, elaborados pelo Conselho Nacional de Controle de Experimentação Animal (CONCEA), sobre a utilização de animais em atividades educacionais e em experimentos que envolvam espécies definidas na Lei 11.794/2008. Este projeto visa determinar valores de referência para espécie contribuindo para a medicina de coelhos a nível mundial.

Após estes esclarecimentos, solicitamos o seu consentimento de forma livre para a participação de seu(s) animal(is). Preencher, por favor, os itens que se seguem:

Consentimento Livre e Esclarecido

Tendo sido orientado quanto ao teor de todo o aqui mencionado e compreendido a natureza e o objetivo do já referido estudo, manifesto meu livre consentimento em participar, estando totalmente ciente de que não há nenhum valor econômico, a receber ou a pagar, por minha participação.

Nome do Proprietário: _____

CPF/RG: _____

Assinatura do Proprietário

Pesquisador responsável

Curitiba, ____/____/____

Journal of Exotic Pet Medicine

Computed tomographic findings of the urinary tract in rabbits (*Oryctolagus cuniculus*) --Manuscript Draft--

Manuscript Number:	JEPM-D-20-00179
Full Title:	Computed tomographic findings of the urinary tract in rabbits (<i>Oryctolagus cuniculus</i>)
Article Type:	Research article
Keywords:	Rabbit; Multidetector computed tomography; Sectional anatomy; Urinary tract
Corresponding Author:	Danielle Buch Universidade Federal do Parana Setor de Ciencias da Agrárias Curitiba, Paraná BRAZIL
Corresponding Author Secondary Information:	
Corresponding Author's Institution:	Universidade Federal do Parana Setor de Ciencias da Agrárias
Corresponding Author's Secondary Institution:	
First Author:	Danielle Buch, DVM
First Author Secondary Information:	
Order of Authors:	Danielle Buch, DVM André Saldanha, Msc Eloisa Muehlbauer, Msc Wesley Júnior de Oliveira, DVM Elaine Mayumi Ueno Gil, Phd Tilde Rodrigues Froes, Phd; Assistant Professor and Chief Residents.
Order of Authors Secondary Information:	
Abstract:	Urinary tract disease is a common reason for presentation of rabbits in small animal clinical practice. The diagnosis of urinary disorders can be challenging due to physiological and anatomical features that distinguish rabbits from other mammals. Multidetector computed tomography may be a useful tool in rabbits, as it is in dogs and cats. The aim of this study was to describe the appearance of the urinary tract in healthy rabbits using computed tomography (CT). Qualitative and quantitative CT evaluation of the urinary tract was made in 23 healthy rabbits under general anesthesia using a soft tissue algorithm and multiplanar reconstructions. In rabbits the distance between the right and left kidney poles is larger than in dogs and cats, with greater kidney mobility within retroperitoneal space. The right kidney can be located between the vertebral bodies of T13 to L2, and the left kidney between the body of L2 and the cranial margins of L5. There was a good interobserver correlation for renal shape, margins, size and attenuation patterns of the organs between the rabbits studied. However, there was interobserver disagreement regarding the measurements of renal pelvis, ureters and the exact position of the kidneys in relation to the lumbar vertebrae. Although the ureters are thin, the ureteral path was well defined by contrast enhancement. However, some focal filling defects were observed in the middle and caudal third of the ureters in more than 50% of the animals. In addition to structural evaluation, CT allows for dynamic and functional evaluation of the urinary tract. CT images are less affected by gastrointestinal changes than other forms of imaging (radiography or ultrasonography). This study provides a detailed anatomic description of the urinary tract in rabbits from CT imaging.
Additional Information:	
Question	Response
Does your submission include Data in	My submission does not include Data in Brief.

Journal of Exotic Pet Medicine

Computed tomographic findings of the urinary tract in rabbits (*Oryctolagus cuniculus*) --Manuscript Draft--

Manuscript Number:	JEPM-D-20-00179R1
Full Title:	Computed tomographic findings of the urinary tract in rabbits (<i>Oryctolagus cuniculus</i>)
Article Type:	Research article
Keywords:	Lagomorphs; Multidetector computed tomography; Sectional anatomy; Urinary system
Corresponding Author:	Danielle Buch Universidade Federal do Parana Setor de Ciencias da Agrárias Curitiba, Paraná BRAZIL
Corresponding Author Secondary Information:	
Corresponding Author's Institution:	Universidade Federal do Parana Setor de Ciencias da Agrárias
Corresponding Author's Secondary Institution:	
First Author:	Danielle Buch, DVM
First Author Secondary Information:	
Order of Authors:	Danielle Buch, DVM André Saldanha, Msc Eloisa Muehlbauer, Msc Wesley Júnior de Oliveira, DVM Elaine Mayumi Ueno Gil, Phd Tilde Rodrigues Froes, Phd; Assistant Professor and Chief Residents.
Order of Authors Secondary Information:	
Abstract:	The diagnosis of urinary disorders can be challenging in rabbits. Although reference values for some characteristics of urinary tract in rabbits already exist in most imaging modalities, almost no studies using multidetector computed tomography (MDTC) are described. The aim of this study was to describe the appearance and the main features of the urinary tract in healthy pet rabbits using computed tomography (CT). Healthy rabbits were scanned under general anesthesia to evaluate the urinary tract. The normal renal length was determined in a range of 3.27-3.43 cm. The ureters were identified in the pre-contrast phase but better delineated in post-contrast phases; however, some focal filling defects were observed in the middle and caudal third of the ureters in more than 50% of the animals in post-contrast exams. Interobserver analysis was performed and disagreement regarding the measurements of renal pelvis, ureters and the exact position of the kidneys in relation to the lumbar vertebrae was observed. Urinary tract structures assessed by CT did not suffer direct interference by gastrointestinal tract compared other forms of imaging (radiography or ultrasonography), in exception to the specific regions of the ureteral path. This study provides a detailed anatomic description of the urinary tract in rabbits from CT imaging and reference values for further investigations.
Response to Reviewers:	
Additional Information:	
Question	Response
Does your submission include Data in Brief? If so, please upload all Data in Brief files (completed Word template and any	My submission does not include Data in Brief.

Journal of Exotic Pet Medicine

Computed tomographic findings of the urinary tract in rabbits (*Oryctolagus cuniculus*) --Manuscript Draft--

Manuscript Number:	JEPM-D-20-00179R2
Full Title:	Computed tomographic findings of the urinary tract in rabbits (<i>Oryctolagus cuniculus</i>)
Article Type:	Research article
Keywords:	Lagomorphs; Multidetector computed tomography; Sectional anatomy; Urinary system
Corresponding Author:	Danielle Buch Universidade Federal do Parana Setor de Ciencias da Agrárias Curitiba, Paraná BRAZIL
Corresponding Author Secondary Information:	
Corresponding Author's Institution:	Universidade Federal do Parana Setor de Ciencias da Agrárias
Corresponding Author's Secondary Institution:	
First Author:	Danielle Buch, DVM
First Author Secondary Information:	
Order of Authors:	Danielle Buch, DVM André Saldanha, Msc Eloisa Muehlbauer, Msc Wesley Júnior de Oliveira, DVM Elaine Mayumi Ueno Gil, Phd Tilde Rodrigues Froes, Phd; Assistant Professor and Chief Residents.
Order of Authors Secondary Information:	
Abstract:	The diagnosis of urinary disorders can be challenging in rabbits. Although reference values for some characteristics of urinary tract in rabbits already exist in most imaging modalities, almost no studies using multidetector computed tomography (MDTC) are described. The aim of this study was to describe the appearance and the main features of the urinary tract in healthy pet rabbits using computed tomography (CT). Healthy rabbits were scanned under general anesthesia to evaluate the urinary tract. The normal renal length was determined in a range of 3.27-3.43 cm. The ureters were identified in the pre-contrast phase but better delineated in post-contrast phases; however, some focal filling defects were observed in the middle and caudal third of the ureters in more than 50% of the animals in post-contrast exams. Interobserver analysis was performed and disagreement regarding the measurements of renal pelvis, ureters and the exact position of the kidneys in relation to the lumbar vertebrae was observed. Urinary tract structures assessed by CT did not suffer direct interference by gastrointestinal tract compared other forms of imaging (radiography or ultrasonography), in exception to the specific regions of the ureteral path. This study provides a detailed anatomic description of the urinary tract in rabbits from CT imaging and reference values for further investigations.
Response to Reviewers:	Dear Reviewers: Abstract was reviewed and structured like the recent JEPM paper. Grammatical/typographical topics of Introduction, material and methods, results and discussion section were adjusted according to your suggestions. Reviewer 1: - Previously concerns about statistical analysis were removed.

Journal of Exotic Pet Medicine

Computed tomographic findings of the urinary tract in rabbits (*Oryctolagus cuniculus*) --Manuscript Draft--

Manuscript Number:	JEPM-D-20-00179R3
Full Title:	Computed tomographic findings of the urinary tract in rabbits (<i>Oryctolagus cuniculus</i>)
Article Type:	Research article
Keywords:	Lagomorphs; Multidetector computed tomography; Sectional anatomy; Urinary system
Corresponding Author:	Danielle Buch Universidade Federal do Parana Setor de Ciencias da Agrárias Curitiba, Paraná BRAZIL
Corresponding Author Secondary Information:	
Corresponding Author's Institution:	Universidade Federal do Parana Setor de Ciencias da Agrárias
Corresponding Author's Secondary Institution:	
First Author:	Danielle Buch, DVM
First Author Secondary Information:	
Order of Authors:	Danielle Buch, DVM André Saldanha, Msc Eloisa Muehlbauer, Msc Wesley Júnior de Oliveira, DVM Elaine Mayumi Ueno Gil, Phd Tilde Rodrigues Froes, Phd; Assistant Professor and Chief Residents.
Order of Authors Secondary Information:	
Abstract:	<p>Background</p> <p>The diagnosis of urinary disorders can be challenging in rabbits. Reference values for some characteristics of the urinary tract in rabbits already exist for most imaging modalities. However, there are few studies describing findings using multidetector computed tomography. The aim of this study was to describe the appearance and main features of the urinary tract in healthy pet rabbits using computed tomography (CT).</p> <p>Methods</p> <p>The urinary tract of 23 healthy rabbits was scanned under general anesthesia pre- and post-contrast injection.</p> <p>Results</p> <p>Normal renal length was 3.27-3.43 cm. The ureters were identified in the pre-contrast phase, but better delineated in post-contrast phases. Some focal filling defects were observed in the middle and caudal third of the ureters in more than 50% of the animals on post-contrast exams. There was interobserver disagreement regarding the measurements of renal pelvis, ureters and the exact position of the kidneys in relation to the lumbar vertebrae.</p> <p>Conclusions and clinical relevance</p> <p>This study provides a detailed anatomic description of the urinary tract in rabbits from</p>